CONTROL, OPTIMIZATION AND MONITORING OF PORTLAND CEMENT (PC 42.5) QUALITY AT THE BALL MILL

A Thesis Submitted to
the Graduate School of Engineering and Sciences of
İzmir Institute of Technology
in Partial Fulfillment of the Requirements for the Degree of

MASTER OF SCIENCE

in Chemical Engineering

by
Hakan AVŞAR

January 2006
İZMİR

We approve the thesis of **Hakan AVŞAR**

Date of Signature

……. **16 January 2006**
Asst. Prof. Dr. Fuat DOYMAZ
Supervisor
Department of Chemical Engineering
İzmir Institute of Technology

…… **16 January 2006**
Assoc. Prof. Dr. Sedat AKKURT
Co-Supervisor
Department of Mechanical Engineering
İzmir Institute of Technology

…….. **16 January 2006**
Asst. Prof. Dr. Fikret İNAL
Department of Chemical Engineering
İzmir Institute of Technology

…….. **16 January 2006**
Asst. Prof. Dr. Serhan ÖZDEMİR
Department of Mechanical Engineering
İzmir Institute of Technology

…….. **16 January 2006**
Prof. Dr. Devrim BALKÖSE
Head of Department
İzmir Institute of Technology

.....
Assoc. Prof. Dr. Semahat ÖZDEMİR
Head of the Graduate School

ACKNOWLEDGEMENTS

I would like to express my sincere gratitude to my advisors, Asst. Prof. Dr. Fuat DOYMAZ and Assoc. Prof. Dr. Sedat AKKURT for their supervision, guidance and encouragement throughout this study.

I am grateful to Çimentaş Cement Company administration for the data used in this study, valuable discussions, and financial support.

Special thanks to my love and all of my friends for their support and understanding.

Finally, I would like to deeply appreciate my family for their help, support, encouragement and understanding throughout my life.

ABSTRACT

In this study, artificial neural networks (ANN) and fuzzy logic models were developed to model relationship among cement mill operational parameters. The response variable was weight percentage of product residue on 32-micrometer sieve (or fineness), while the input parameters were revolution percent, falofon percentage, and the elevator amperage (amps), which exhibits elevator charge to the separator.

The process data collected from a local plant, Cimentaş Cement Factory, in 2004, were used in model construction and testing. First, ANN (Artificial Neural Network) model was constructed. A feed forward network type with one input layer including 3 input parameters, two hidden layer, and one output layer including residue percentage on 32 micrometer sieve as an output parameter was constructed. After testing the model, it was detected that the model's ability to predict the residue on 32-micrometer sieve (fineness) was successful (Correlation coefficient is 0.92).

By detailed analysis of values of parameters of ANN model's contour plots, Mamdani type fuzzy rule set in the fuzzy model on MatLAB was created. There were three parameters and three levels, and then there were third power of three (27) rules. In this study, we constructed mix of Z type, S type and gaussian type membership functions of the input parameters and response. By help of fuzzy toolbox of MatLAB, the residue percentage on 32-micrometer sieve (fineness) was predicted. Finally, It was found that the model had a correlation coefficient of 0.76.

The utility of the ANN and fuzzy models created in this study was in the potential ability of the process engineers to control processing parameters to accomplish the desired cement fineness levels.

In the second part of the study, a quantitative procedure for monitoring and evaluating cement milling process performance was described. Some control charts such as CUSUM (Cumulative Sum) and EWMA (Exponentially Weighted Moving Average) charts were used to monitor the cement fineness by using historical data. As a result, it is found that CUSUM and EWMA control charts can be easily used in the cement milling process monitoring in order to detect small shifts in 32-micrometer fineness, percentage by weight, in shorter sampling time interval.

ÖZET

Bu çalışmada, çimento değirmeni işletme parametreleri arasındaki ilişkiyi modellemek için yapay sinir şebekeleri ve bulanık mantık modelleri geliştirilmiştir. Çıkış değişkeni olarak 32 mikrometre eleğin üzerinde kalan ürünün ağırlıkça yüzdesi (incelik) alınırken, giriş parametreleri olarak devir yüzdesi, falofon yüzdesi ve elevatörden ayırıcıya giden maddenin miktarını gösteren elevatör akımı alınmıştır.
Çimentaş çimento fabrikasından 2004 yılına ait işletme verisi model kurumu ve test için kullanılmıştır. İlk olarak, Yapay Sinir Ağları modeli kurulmuştur. Üç giriş parametresini içeren bir giriş, iki gizlenmiş ve 32 mikrometre elek üzerinde kalan ürün (ağırlıkça yüzde) çıkış parametresi olarak içeren bir çıkış tabakasından oluşan bir ileri besleme ağından oluşturulmuştur. Model test edildikten sonra modelin 32 mikrometre inceliği tahmin etme yeteneğinin yüksek olduğu tespit edilmiştir (Düzeltme katsayısı 0,92 bulunmuştur.).

Model üzerinde hassaslık analizi sonucunda karşılık kontur grafikleri giriş parametreleri kullanılarak oluşturulmuştur. Yapay Sinir Ağları modelinin karşılık kontur grafiklerinin parametre değerleri detaylı incelenmesiyle MatLAB'daki bulanık modelde Mamdani tipinde bulanık kural seti oluşturulmuştur. Üç parametre ve üç seviye olduğu için üç üzeri üç (27) kural vardır. Bu çalışmada, Z, S ve gauss tipindeki üyelik fonksiyonlarının karışımı ile oluşturulmuştur. MatLAB kullanım kutusunun yardımı ile 32 mikrometre incelik (ağırlıkça yüzde) tahmin edilmiştir. Sonuç olarak, modelin düzeltme katsayısı (R) 0,76 bulunmuştur.

Bu çalışmada oluşturulan YSA ve bulanık modeller, işletme mühendislerine istenilen çimento inceliğine ulaşmak için işletme parametrelerini kontrolünde potansiyel yeterlilikte yarar göstermektedir.

Çalışmamızın ikinci kısmında, çimento öğütüm sürecinin performansını değerlendirmek ve süreci denetlemek için nicel bir izlek tanımlanmıştır. Tarihsel veri kullanılarak, CUSUM (gittikçe artan toplam) ve EWMA (üssel ölçülmüş hareketli ortalama) grafikleri gibi kontrol grafikleri çimento inceliğini denetlemek için kullanılmıştır. Sonuç olarak, CUSUM ve EWMA kontrol grafiklerinin 32 mikrometre inceliğindeki, (ağırlıkça yüzde) küçük sapmaları tespit etmek için çimento öğütüm sürecinde daha kısa süreli örnek alım zaman aralıklarında kolayca kullanılabileceği bulunmuştur.

TABLE OF CONTENTS

LIST OF FIGURES

LIST OF TABLES

CHAPTER 1

INTRODUCTION

Cement is a finely ground inorganic material, which, when mixed with water, forms a paste which hardens by means of hydration reactions and which, after hardening, retains its strength and stability even under water.

Quality of cement, mostly, is resembled by mortar compressive strength. Chemical structure, fineness and particle size distribution of finished product have a strong influence on mortar compressive strength. European and American Standards accept fineness, which has considerable effects on cement strength and hydration rate, as a vital parameter. As an example, in fine cement, more gypsum is required for proper retardation because increasing fineness makes more tricalcium aluminate available for early hydration. And, higher early rate of hydration causes higher early rate of heat liberation, which may cause cracking in concrete constructions. Finally, grinding feed to very fine particles requires more energy, increasing the production cost. On the other hand, smaller particle size lets the more area available for water-cement interaction per unit volume. The finer particles (up to 8 micrometer) dominate the early strength development of the cement (up to 2 days) while the larger particles dominate the strength after this time (PCA 1988). Due to these facts, variation of cement fineness should be well controlled and monitored during the cement milling process.

The cement milling process is a complex process that involves many parameters affecting the quality parameter of weight percentage of product residue on sieve (or fineness) with definite size of holes.

An analytical model to describe the effects of each of these factors on fineness can be very complex. Artificial neural networks (ANN) and fuzzy logic can be used for this purpose as a tool for prediction modelling of fineness. Its use for cement tube mill was previously studied (Topalov and Kaynak 1996) for preventing mill from plugging. In addition, the analysis and optimization of the cement grinding circuits were performed with the application of the Bond based methodology as well as Population Balance Models (PBM) (Jankovic 2004). In the literature, several control approaches have been proposed including linear multivariable control techniques. Applications of

ANN (Grognard 2001) and fuzzy logic models (Akyol et al. 2003) were previously used for cement strength prediction. However, the use of fuzzy logic and ANN modelling for cement fineness prediction has not yet been reported.

In this study, our objectives are to predict the fineness before any variations in process parameters, to decrease the errors arisen from the operators, to increase the efficiency and finally decrease the process cost. In order to get these targets, residue on 32-μm sieve (or fineness) of portland cement is to be predicted by using Tube Mill operational parameters: revolution "%" (instant rotational speed x 100 / max rotational speed), falofon "%" (instant media and feed charge/max charge), and elevator amperage "A". For this purpose, cement milling process in a local plant was modelled by using Artificial Neural Networks and Fuzzy Logic approaches. The data were collected from the local plant that uses fineness test as a process control parameter between the months of January and December 2004.

Two combined modelling studies were performed using this data. First, the ANN on MatLAB® was applied by using operational parameters such as Revolution "%", Falofon "%" and Elevator Amperage "A". The response surfaces of the ANN model were used to construct the Mamdani-type fuzzy rule set in the fuzzy model on MatLAB®. Finally, the view of rule set and start-up, which were used to predict 32-μm fineness of cement, were obtained.

In order to monitor 32-μm fineness, % wt, of cement, the local plant applies basic Individual Control Chart. However, it has been observed that the chart does not correspond small shifts. If the high production rate (180 t/h) and effect of fineness on the quality of cement mortar are considered, these shifts lead serious problems with the cement stocked in the silos with capacity of 10.000 t. Hence, in the second part of our study, I-MR (Individual Moving Range) control chart, CUSUM (Cumulative Sum), EWMA (Exponentially Weighted Moving Average) and MA (Moving Average) control chart were applied in order to detect small shifts in cement fineness, which is one of quality parameters of the milling process. The performances of these control charts were compared.

In chapter 2, cement-manufacturing process is described, briefly. Cement manufacturing process is composed of four main steps: quarrying and raw materials preparation, clinker burning, grinding of cement clinker, and finally, packing and dispatch of cement.

In chapter 3, the types of portland cement (EN and ASTM) are to be mentioned. In addition to this, chemical composition of portland cement is defined. Finally, some information about physical properties of portland cement such as fineness and compressive strength is given.

In chapter 4, in order to get clear visual, some brief information about Artificial Intelligence Systems is to be given. Network Architectures and Learning Processes are discussed in Artificial Neural Networks part. In Fuzzy Logic part, fundamentals of Fuzzy Sets and Fuzzy Logic Approach are to be discussed.

In chapter 5, cement-milling process and parameters affecting on fineness are explained.

In chapter 6, construction of ANN models that were created in the thesis is explained.

In chapter 7, the results of the model created in this study are discussed.

In chapter 8, statistical monitoring of quality parameter of 32-μm fineness of portland cement is explained.

CHAPTER 2

CEMENT MANUFACTURING PROCESS

Portland cement is produced by grinding cement clinker in association with gypsum (3-5 %) to specified fineness depending on the requirements of the cement consumers. Cement clinker is produced on large scale by heating finely ground raw materials (Calcareous and Argillaceous materials) at very high temperature up to 1450 ^{o}C in rotary kilns. The materials that can be used in cement industry as raw materials are listed in Table 2.1.

Table 2.1. Raw materials used in cement industry.

CaO Source	**Silica-SiO_2 Source**	**Alumina-Al_2O_3 Source**	**Iron-Fe_2O_3 Source**
Limestone	Clay	Clay	Clay
Marble	Shale	Bauxite	Iron Ore
Marl	Marl		
Calcite	Sand		
Chalk	Quartzite		

Calcareous and Argillaceous obtained from the earth are properly proportioned in order to get a suitable ratio of lime (CaO), Silica (SiO_2), Alumina (Al_2O_3) and Iron (Fe_2O_3) present in the mixture. As the raw materials are obtained directly from limestone and clay mines, minor constituents like Magnesia (MgO), Sodium, Potassium, Sulphur, Chlorine compounds etc., may also be present in the raw materials up to limited extent which do not adversely affect either the manufacturing process or the quality of cement produced. As a major raw material limestone is used for manufacture of cement. Due to this fact, a cement unit is necessarily located near the cement grade limestone deposit. If it is considered that 25-35 % of raw materials is lost

in the atmosphere in the form of gaseous compounds such as carbon dioxide and nitrogen oxides, the location of a cement unit near the deposits is seen as a vital aspect in cement manufacturing process. Figure B1 represents a typical dry process of cement production flow chart.

Major unit operations involved in cement manufacturing process include:

- Quarrying and Raw Materials Preparation.
- Clinker burning
- Grinding of cement clinker
- Packing and dispatch of cement.

In the following sections, we will be discussing these unit operations.

2.1. Quarrying and Raw Materials Preparation

Major quantity of limestone is obtained from the captive limestone mines of the plant. However, depending upon the proportions of different cement clinker phase forming components, additive materials including high grade / low grade limestone can be purchased from outside parties in required quantities in order to obtain the desired quality of cement grade raw meal.

Big boulders, which are produced during drilling and blasting methods of limestone mining, are crushed in suitable type of crushers. The crushing is carried out either in single or double stages by using Primary crusher and Secondary crusher, or in a single stage crushing machine depending upon the size of the boulder produced from mining. This also depends on the type of grinding mills used for grinding raw materials for preparation of finally pulverized raw meal. A jaw hammer crusher is used in Çimentaş Cement Company for size reduction of limestone boulders to a suitable feed size. Such crusher was installed at the plant site. Limestone produced in the mine is transported to crusher site with the help of dumpers. Crushed limestone is then transported to plant stockpile with the help of Belt conveyor.

Crushed limestone is then transported to stacker reclaimer site with the help of belt conveyor / rope ways installed at different sites of the plant. Finally, crushed limestone is pre-blended with the help of stacker and reclaimer systems. Crushed limestone traveling on the belt conveyors is stacked in layers with the help of stacker machine. Stacked materials is then cut in slices with the help of a reclaiming machine

which mixes layers of stacked limestone to reduce the variation in quality of limestone relative to large variations seen in the limestone ore.

The pre-blended limestone from stack pile is then transported to raw mill hoppers. More than one hoppers are used for proportioning of raw mix incase the limestone is obtained from several sources or additive materials required to be mixed with captive mines of limestone. Presently, raw mill hoppers are provided with continuous weighing machines known as weigh feeders in order to produce a suitable raw meal proportioned appropriately for production of desired good quality of cement clinker. Vertical Roller Mill and Tube Mill Grinding machines are used for production of pulverized raw meal at the company.

2.2. Clinker Burning

Portland cement clinker is produced from a mixture of raw materials containing calcium, silicon, aluminum, and iron as the main elements. The mixture is heated in kilns that are long rotating steel cylinders on an incline. The kilns may be up to 6 meters in diameter and 180 meters in length. Mixture of raw materials enters at the high end of the cylinder and slowly moves along the length of the kilns due to the constant rotation and inclination. At the low end of the kilns, fuel is injected and burned, thus providing the heat necessary to make the materials react. It can take up to 2 hours for the mixture to pass through the kiln, depending upon the length of the cylinder.

When mixed in correct proportions, new minerals with hydraulic properties – the so-called clinker phases – are formed upon heating up to the sintering (or clinkerization) temperature as high as 1450° C. The main mineral components in clinker are silicates, aluminates and ferrites of the element calcium. The main clinker phases are listed in Table 2.2 .

Table 2.2. Phases of clinker

Tri-Calcium silicate	3 $CaO.SiO_2$	C_3S	Alite
Di-Calcium silicate	2 $CaO.SiO_2$	C_2S	Belite
Tri-Calcium aluminate	3 $CaO.Al_2O_3$	C_3A	Aluminate Phase
Calcium Alumina ferrite	4 $CaO.Al_2O_3.Fe_2O_3$	C_4AF	Brownmillerite

The clinker formation process can be divided into four main steps (Figure 2.1):

- **Drying and preheating** (20 – 800° C): release of free and chemically bound water
- **Calcination** (800 – 1350° C): release of CO_2: initial reactions with formation of clinker minerals and intermediate phases. Conversion of $CaCO_3$ to CaO and $MgCO_3$ to MgO.
- **Sintering or clinkerization** (1350 – 1550° C): formation of calcium silicates, calcium aluminates and liquid phase
- **Kiln internal cooling** (1550 – 1200° C): crystallization of calcium aluminate and calcium ferrite

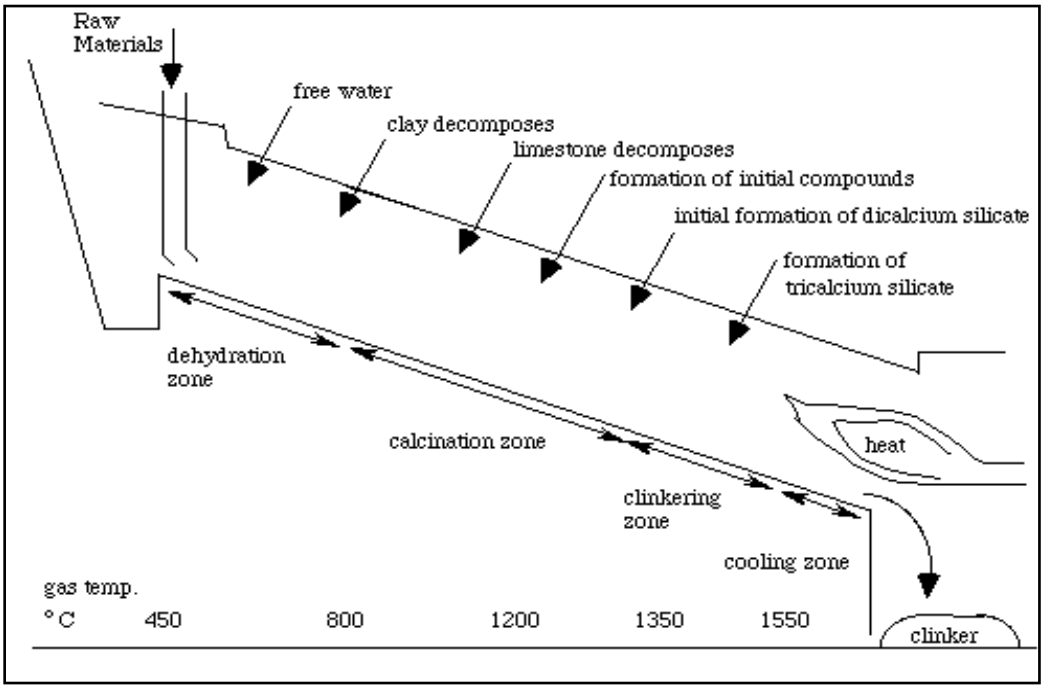

Figure 2.1. Schematic diagram of rotary kiln.

As the mixture moves down the cylinder, it progresses through four stages of transformation. Initially, any free water in the powder is lost by evaporation. Next, decomposition occurs from the loss of bound water and carbon dioxide. This is called calcination. The third stage is called clinkerisation. During this stage, the calcium silicates are formed. The final stage is the cooling stage.

The marble-sized pieces produced by the kiln are referred to as **clinker**. Clinker is actually a mixture of four compounds as illustrated in Table 2.2. The clinker is cooled with the help of grill cooler in order to get it to stable phases.

2.3. Grinding of Cement Clinker

In order to achieve the objectives of energy conservation, the clinker produced in rotary kiln cooled in cooler is usually stored for few days before it is ground in cement grinding mills along with appropriate quantity of gypsum and other additive materials for production of finely pulverized cement with desired fineness. Fineness and particle size distributions of the finished product have a strong influence on the cement quality.

Ball / Tube mills (in open circuit or closed circuit mode) are generally used for clinker grinding in cement plant worldwide.

Blended cements (or “composite” cements) contain other constituents in addition such as granulated blast-furnace slag, natural or industrial puzzolan (for example, volcanic tuff or fly ash from thermal power plants), or inert fillers such as limestone.

Mineral additions in blended cements may either be inter-ground with clinker or ground separately or mixed with Portland cement.

The tube mill consists of a steel cylindrical shell with three compartments. The first compartment is used for drying of the raw material in order to increase the performance of the milling by removing water from the raw material. The following compartments include steel balls with different dimensions. In the second compartment, raw materials (clinker and additive materials) are pre-milled by the help of big steel balls having a radius of 60-90 mm. By using balls of smaller radius, size of pre-milled material is reduced down to maintain desired level of fineness of the finished product. A dynamic separator is used for differentiate the fine and thick particles coming from the

mill exit. The fine particles are sent to the silos as finish product (cement). The remaining part (thick particles) is recycled to the mill for re-milling. In Chapter 5, Process parameters and standards will be more elaborated.

2.4. Packing and Dispatch of Cement

The pulverized different types of cements are stored in different silos installed with different capacities. Depending upon the customer requirements, cement is loaded in bulk, or in 50 kg bags that are packed with the help of conventional rotary packaging or electronic packaging equipment, and finally loaded onto trucks that are dispatched to final destinations.

CHAPTER 3

PORTLAND CEMENT

Portland cement is the chief ingredient in cement paste - the binding agent in Portland cement concrete (PCC). It is a hydraulic cement that, when combined with water, hardens into a solid mass. Interspersed in an aggregate matrix it forms PCC. As a material, portland cement has been used for well over 175 years and, from an empirical perspective, its behavior is well understood. The patent for portland cement was obtained in 1824 by Joseph Aspdin. Chemically, however, portland cement is a complex substance whose mechanisms and interactions have yet to be fully defined. The Portland Cement Association (PCA) provides the following precise definitions:

Hydraulic cement: Hydraulic binder, ie. a finely ground inorganic material, which, when mixed with water, forms a paste which sets and hardens by means of hydration reactions and processes and which, after hardening, retains its strength and stability even under water.

Portland cement: An hydraulic cement composed primarily of hydraulic calcium silicates.

3.1. Background

Although the use of cements (both hydraulic and non-hydraulic) goes back many thousands of years (to ancient Egyptian times at least), the first occurrence of "portland cement" came about in the 19th century. In 1824, Joseph Aspdin, a Leeds mason took out a patent on a hydraulic cement that he coined "portland" cement. He named the cement because it produced a concrete that resembled the color of the natural limestone quarried on the Isle of Portland, a peninsula in the English Channel. Since then, the name "portland cement" has stuck and is written in all lower case because it is now recognized as a trade name for a type of material and not a specific reference to Portland, England.

Today, portland cement is the most widely used building material in the world with about 1.56 billion tones (1.72 billion tons) produced each year. Annual global production of portland cement concrete hovers around 3.8 million cubic meters (5 billion cubic yards) per year (Cement Association of Canada, 2004).

3.2. Types of Portland Cement

Portland cement is hydraulic cement produced by milling clinker, which includes calcium silicates, calcium aluminates with calcium sulphate as an additive. Due to the fact that its low cost and widespread availability of its raw material, limestone, portland cement one of the materials widely used. In order to meet different physical and chemical requirements for specific purposes, such as durability and high-early strength, different types of portland cement are manufactured. American Society for Testing Materials (ASTM), and European Standards (EN) exhibit some differences.

3.2.1. Portland Cement (American Standard Type)

Eight types of cement are covered in ASTM C 150. These types and brief descriptions of their uses are listed in Table 3.1.

Table 3.1. Portland cement types and their uses

Cement type	Use
I	General purpose cement, when there are no extenuating conditions
II	Aids in providing moderate resistance to sulfate attack
III	When high-early strength is required
IV	When a low heat of hydration is desired
V	When high sulfate resistance is required
IA	A type I cement containing an integral air-entraining agent
IIA	A type II cement containing an integral air-entraining agent
IIIA	A type III cement containing an integral air-entraining agent

3.2.2. Portland Cement (European Standard Types)

EN standards use two types of Portland cement:

CEM I: Portland Cement

CEM II: Composite-Portland Cement

The company, ÇİMENTAŞ, uses CEM I type Portland cement for general purposes.

3.3. Chemical Composition of Portland Cement

Portland cements can be characterized by their chemical composition although they rarely are for pavement applications. However, it is a portland cement's chemical properties that determine its physical properties and how it cures. Therefore, a basic understanding of portland cement chemistry can help one understand how and why it behaves as it does. On the basis of quantity, the constituents of portland cement can be categorized into:

- Major constituents
- Minor constituents

The composition of portland cements is what distinguishes one type of cement from another. The major constituents in portland cement are denoted as tricalcium silicate (C_3S), dicalcium silicate (C_2S), tricalcium aluminate (C_3A), and tetracalcium aluminoferrite (C_4AF). The actual components are often complex chemical crystalline and amorphous structures, denoted by cement chemists as "elite" (C_3S), "belite" (C_2S), and various forms of aluminates. Tricalcium silicate and dicalcium silicate, significantly, contribute to the strength of hydrated cement paste. The roles of tricalcium aluminate and tetracalcium aluminoferrite in strength development are controversial (Bogue 1955). Tricalcium aluminate contributes to flash setting. However, gypsum retards this effect, allowing tricalcium silicate set first. Otherwise a rather porous calcium aluminate hydrate would form, providing the remaining cement compounds a porous framework for hydration – adversely affecting the strength of the cement paste (Taylor, 1964).

The behavior of each type of cement depends on the content of these components. Main Constituents in a typical portland cement is exhibited in Table 3.3.

Table 3.2. Main Constituents in a typical portland cement (Mindess et al. 1990).

Chemical Name	Chemical Formula	Shorthand Notation
Tricalcium Silicate	$3CaO.SiO_2$	C_3S
Dicalcium Silicate	$2CaO.SiO_2$	C_2S
Tricalcium Aluminate	$3CaO.Al_2O_3$	C_3A
Tetracalcium Aluminoferrite	$4CaO.Al_2O_3.Fe_2O_3$	C_4AF
Gypsum	$CaSO_4.H_2O$	CSH_2

3.4. Physical Properties of Cements

EN and ASTM standards have specified certain physical requirements for each type of cement. These properties include:

1) Fineness
2) Setting time
3) Soundness
4) Compressive strength
5) Heat of hydration
6) Loss of ignition.

3.4.1. Fineness

Fineness is defined depending upon the method of measurement. It may be defined as sieve diameter: the width of the minimum square aperture through which particle pass, or surface diameter: diameter of sphere having the same surface as the surface of particle. Fineness of portland cement has great effects on hydration rate and thus the setting time, the rate of strength gain. As an example, the smaller is the particle size, the greater the surface area-to-volume ratio. This causes more area available for water-cement interaction. The finer particles mainly affect the early strength of the cement (2 days) while the larger particles dominate the strength after this time. The

effects of greater fineness on strength are generally seen during the first seven or twenty eight days (Czernin 1980).

There are, however, several disadvantages associated with high fineness:

- In fine cement, more gypsum is required for proper retardation because increased fineness makes more tricalcium aluminate available for early hydration.
- Grinding clinker to a high fineness requires more energy, increasing the production cost.
- A higher early rate of hydration causes a higher early rate of heat liberation. If not properly dissipated, this heat may cause cracking – especially in mass concrete construction.
- The reaction of fine cement with alkali-reactive aggregate is stronger.

Fineness, which has considerable effects on cement strength and hydration rate, is accepted as a vital parameter by European and American Standards.

Fineness can be measured by several methods. Some methods are as follows;

- Fineness of Portland Cement by the Turbidimeter.
- Fineness of Hydraulic Cement by the 90-μm and 32-μm Sieves
- Fineness of Hydraulic Cement by Air Permeability Apparatus (Blaine)

The Wagner Turbidimeter and the Blaine air permeability test for measuring cement fineness is required by the American Society for Testing Materials (ASTM).

Another test to determine the fineness is Sieve Analysis. The fineness of cement is measured by sieving it on standard sieves. The proportion of cement of which the grain sizes are larger than the specified size is thus determined (EN 196-6). The result is recorded as percentage (%). According the local plant specifications, 32-μm sieve fineness of portland cement ranges from 14 % to 19 % by weight. The sieve equipment, which is used in the local plant, is exhibited in Figure B2.

3.4.2. Setting Time

Setting is defined as change of cement paste from a fluid to a rigid state. It occurs as a result of the hydration of cement compounds. Cement paste setting time is affected by cement fineness, water-cement ratio, chemical content. Setting tests are applied to characterize how a cement paste sets.

Normally, two setting times are defined (Mindess and Young 1981):

1. *Initial set*. Occurs when the paste begins to stiffen considerably.
2. *Final set*. Occurs when the cement has hardened to the point at which it can sustain some load.

3.4.3. Soundness

After setting, if the cement paste undergoes substantial volume changes, disruption of the hardened paste could result due to restraints. When referring to Portland cement, "soundness" refers to the ability of a hardened cement paste to retain its volume after setting without delayed destructive expansion (PCA 1988). Excessive amounts of free lime (CaO) or magnesia (MgO) causes this destructive expansion. Most portland cement specifications limit magnesia content and expansion. The typical expansion test places a small sample of cement paste into an autoclave (a high pressure steam vessel). ASTM C 150, *Standard Specification for Portland Cement* specifies a maximum autoclave expansion of 0.80 percent for all portland cement types.

3.4.4. Compressive Strength

Cement paste strength is typically defined in three ways: compressive, tensile and flexural. These strengths can be affected by a number of items including: water-cement ratio, cement-fine aggregate ratio, type and grading of fine aggregate, manner of mixing and molding specimens, curing conditions, size and shape of specimen, moisture content at time of test, loading conditions and age (Mindess and Young 1981). Since cement gains strength over time, the time at which strength test is to be conducted must be specified. In strength tests on cement, the aggregate dimension is eliminated by use of standard aggregates.

Typically times are 2 days (for high early strength cement), 7 days, 28 days (for low heat of hydration cement). When considering cement paste strength tests, there are two items to consider:

- Cement mortar strength is not directly related to concrete strength. Cement paste strength is typically used as a quality control measure.
- Strength tests are applied on cement mortars (cement + water + sand).

The most common strength test, compressive strength, is carried out on a 50 mm cement mortar test specimen. The test specimen is subjected to a compressive load (usually from a hydraulic machine) until failure. This loading sequence must take no less than 20 seconds and no more than 80 seconds.

3.4.5. Heat of Hydration

Hydration is the process by which portland cement, in the presence of water, becomes a bonding agent, evolving heat. In the water-cement paste, the silicates and the aluminates form the products of hydration. With time, they produce a firm and hard mass. The hydrated cement paste is stable in contact with water. The rate of hydration drops with time and, as a result, there can remain a significant amount of unhydrated cement even after a long time.

The heat of hydration is the heat generated when water and portland cement react. Hydration begins at the surface of the cement particles. Therefore, the total surface area of cement represents the material available for hydration. That is, the early rate of hydration depends on the fineness of the cement particles. However, at later stages, the effect of surface area diminishes and, consequently, fineness exercise no influence on the total heat of hydration. Heat of hydration is also influenced by the proportion of C_3S and C_3A in the cement, water-cement ratio, fineness and curing temperature. As each one of these factors is increased, heat of hydration increases. In large mass concrete structures such as gravity dams, hydration heat is produced significantly faster than it can be dissipated (especially in the centre of large concrete masses), which can create high temperatures in the centre of these large concrete masses that, in turn, may cause undesirable stresses as the concrete cools to ambient temperature. Conversely, the heat of hydration can help maintain favorable curing temperatures during winter (PCA 1988).

3.4.6. Loss on Ignition

Loss on ignition is calculated by heating up a cement sample to 900–1000 ^{o}C until a constant weight is obtained. The weight loss of the sample due to heating is then determined. A high loss on ignition can indicate pre-hydration and carbonation, which

may be caused by improper and prolonged storage or adulteration during transport or transfer.

3.5. Influence of Cement on Concrete Properties

Effects of cement on the most important concrete properties are presented in Table 3.3. Cement composition and fineness play a major role in controlling concrete properties. Fineness of cement affects the placability, workability, and water content of a concrete mixture much like the amount of cement used in concrete does.

Table 3.3. Effects of cements on concrete properties (WEB_1 2004).

Cement Property	**Cement Effects**
Placeability	Cement amount, fineness, setting characteristics
Strength	Cement composition (C_3S, C_2S and C_3A), loss on ignition, fineness
Drying Shrinkage	SO_3 content, cement composition
Permeability	Cement composition, fineness
Resistance to sulfate	C_3A content
Alkali Silica Reactivity	Alkali content
Corrosion of embedded steel	Cement Composition (esp. C_3A content)

CHAPTER 4

ARTIFICAL INTELLIGENCE SYSTEMS

The “artificial intelligence” (A.I), in its broadest sense, encompasses a number of technologies that includes, but is not limited to, expert systems, neural networks, genetic algorithms, fuzzy logic systems, cellular automata, chaotic systems, and anticipatory systems.

In data (or information) processing, the objective is generally to gain an understanding of the phenomena involved and to evaluate relevant parameters quantitatively. As an example, it is used in determining the relevant parameters of the cement ball mill. This task is accomplished through modeling of the system, either experimentally or analytically. Most hybrid systems relate experimental data to systems or model. Once, a model of system is obtained, lots kinds of procedure such as sensitivity analysis, statistics regression to have a better understanding of the system are carried out.

Neural networks and fuzzy systems represent two distinct methodologies that deal with uncertainty. Uncertainties that are important include both those in the model, or descriptions of the systems are involved as well as those in the variables. These uncertainties usually arise from complexity (e.g. non-linearity). Neural networks approach the modeling representation by using precise inputs and outputs, which are used to train a generic model which has sufficient degrees of freedom to formulate a good approximation of the complex relationship between the inputs and outputs. Neural network and fuzzy logic technologies are different, and each has unique capabilities that are useful in information processing. Yet, they often can be used to accomplish the same results in a different ways.

4.1. Artificial Neural Networks

Neural networks are good at doing what computers traditionally do not do well, pattern recognition. They are good for sorting data, classifying information, speech

recognition, diagnosis, and predictions of non-linear phenomena. Neural nets are not programmed but learn from examples either with or without supervised feedback.

4.1.1. Background

McCulloch and Pitts, in 1943, proved that networks comprised of neurons could represent any finite logical expression. In 1949 Hebb defined a method for updating the weights in neural networks. Kolmogorov's Theorem was published in the 1950's. It states that any mapping between two sets of numbers can be exactly done with a three-layer network. He did not refer to neural networks in his paper, and this was applied later. His paper also describes how the neural network is to be constructed. The input layer has one neuron for every input. These neurons have a connection to each neuron in the hidden layer. The hidden layer has (2n + 1) neurons (n: the number of inputs). The hidden layer sums a set of continuous real monotonically increasing functions, like the sigmoid function. The output layer has one neuron for every output. Rosenblatt in 1961 developed the Perception ANN (artificial neural network). Then, Widrow and Hoff developed Adaline. 1969 was the year neural networks almost died. A paper published by Minsky and Papert showed that the XOR function could not be done with the Adeline and other similar networks. The 1970's brought NEOCOGNItrON for visual pattern recognition. Hopfield published PDP ("Parallel Distributed Processing") in three volumes.

4.1.2. Human Brain and ANN

ANNs are indeed self-learning mechanisms which don't require the traditional skills of a programmer. Neural networks are composed of simple elements operating in parallel. The main processing element is named as neuron. These elements are inspired by biological nervous systems. In its most general form, a neural network is a machine that is designed to model the way in which the brain performs a particular task or function of interest. Figure 4.1 represents the similarities between human neuron and an artificial neuron.

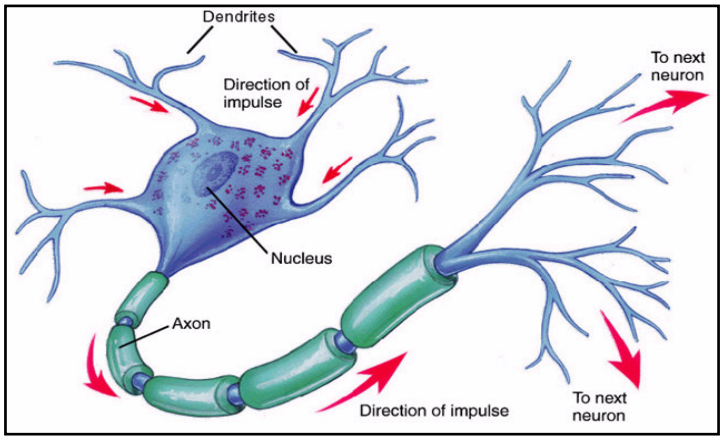

(a)

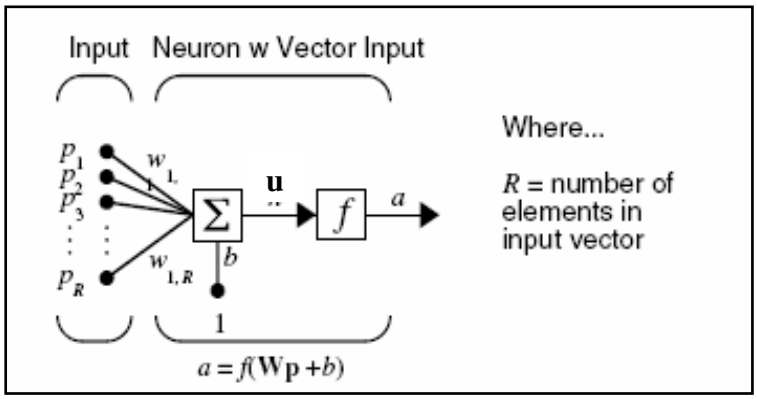

(b)

Figure 4.1. Schematic representations: (a) a human neuron, (b) an artificial neuron. (Source: H. Demuth 2004)

The input signals (p_i), which are taken through dendrites, are multiplied by weights ($w_{i,j}$). The weighted values are fed to the nucleus to be summed as a net function (u). Then, the result is transferred by a transfer function (f (u)) with an activation value (a), to the next neuron through axon. The bias may be simply added to the product *wp* as shown by the summing junction or as shifting the function *f* to the left by an amount *b*. The bias is much like a weight, except that it has a constant input of 1. It is an adjustable (scalar) parameter of the neuron. It is *not* an input.

4.1.3. Mathematical Ways of Describing Neuron

Net function is the summation of weighted values of inputs. It helps describing a neuron in mathematical terms. Two net functions, Linear-basis and Radial-basis function are very important. Linear-basis function (Eqn. 4.1) is the summation of the weighted input values. Radial-basis function (Eqn. 4.2) is the root square of summation of square of difference between input and weight.

$$u_i(w,p) = \sum_{j=1}^{R} w_{ij} p_j \qquad \text{Eqn. 4.1}$$

$$u_i(w,p) = \sqrt{\sum_{j=1}^{R} (p_i - w_{ij})^2} \qquad \text{Eqn. 4.2}$$

The activation function defines the output of a neuron in terms of the induced local field n. There are many transfer or activation functions. Here, we define five basic types of activation functions: hard-limit activation function, linear activation function, sigmoid activation function and tangent-sigmoidal activation function.

The Hard-Limit Function (Eqn 4.3) limits the output of the neuron to either 0, if the net input argument *n* is less than 0; or 1, if *n* is greater than or equal to 0.

$$f(u_i) = \begin{cases} 0 & if\_u_i \le 0 \\ 1 & if\_u_i \ge 0 \end{cases} \qquad \text{Eqn. 4.3}$$

The Linear Function calculates the output by Eqn.4.4. Linear approximations are obtained at the end of neurons, which use this type of activation function.

$$f(u_i) = \alpha u_i \qquad -1 \le f(u_i) \le +1 \qquad \text{Eqn. 4.4}$$

The Sigmoid Function (Eqn.4.5) produces outputs in the interval of (0 to 1). Its function is non-decreasing and monotonic.

$$f(u_i) = \frac{1}{1 + e^{-u_i/\sigma}} \qquad \text{Eqn. 4.5}$$

Alternatively, multilayer networks may use the tan-sigmoid activation (Eqn. 4.6);

$$f(u_i) = \tan sig(u_i) \qquad \text{Eqn. 4.6}$$

4.1.4. Network Architectures

Neural networks, usually, are composed of three layers, input, hidden, and output. More layers can be added, but usually little is gained from doing so. The connections vary by the network type. Some nets have connections from each node in one layer to the next, some have backward connections to the previous layer and some have connections with in the same layer. Neural networks map sets of inputs to sets of outputs. First consider a single layer of neurons.

4.1.4.1. One-Layer of Neurons

A one-layer network with *R* input elements and *S* neurons are as follow;

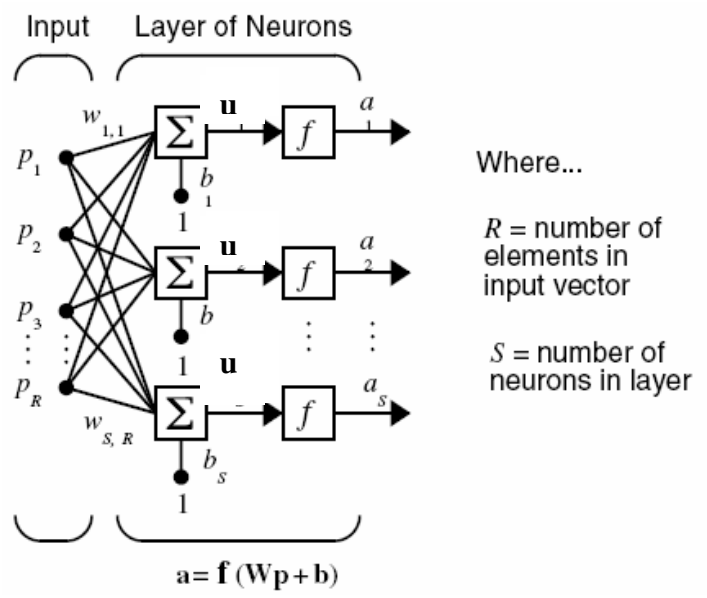

Figure 4.2. A one-layer network with *R* input elements and *S* neurons.
(Source: H. Demuth 2004)

In this network, each element of the input vector **p** is connected to each neuron input through the weight matrix **W**. The i^{th} neuron has a summer that gathers its weighted inputs and bias to form its own scalar output *u(i)*. The various u*(i)* taken together form an *S*-element net input vector **u**. Finally, the neuron layer outputs form a column vector **a**.

4.1.4.2. Multiple Layers of Neurons

A network can have several layers. Each layer has a weight matrix **W**, a bias vector **b**, and an output vector **a**. You can see the use of this layer notation in the three-layer network shown in Figure 4.3.

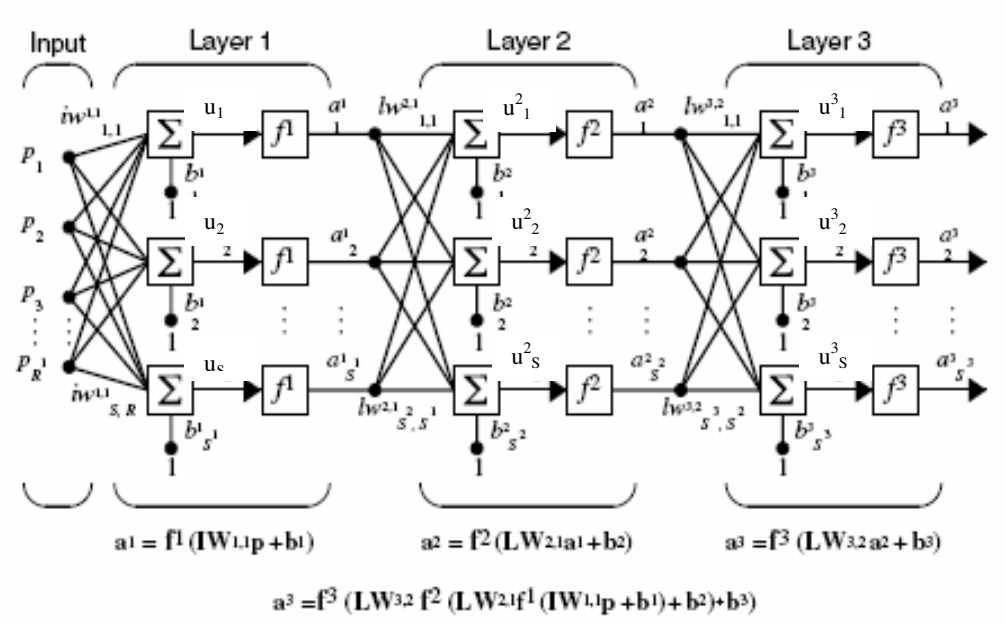

Figure 4.3. A three-layer network with *R* input elements and *S* neurons.
(Source: H. Demuth 2004)

4.1.5. Learning Processes

Learning is a process by which the free parameters of a neural network are adapted through a process of stimulation by the environment in which the network is embedded.

We can define a *learning rule* as a procedure for modifying the weights and biases of a network. There are five basic rules (learning algorithm): error-correction learning, memory-based learning (Back-propagation, BP), Hebbian learning, competitive learning and Boltzmann learning. One of the most widely used learning algorithms is Back-propagation (BP) learning.

Backpropagation was created by generalizing the Widrow-Hoff learning rule to multiple-layer networks and non-linear differentiable transfer functions. Input vectors and the corresponding target vectors are used to train a network until it can approximate a function, associate input vectors with specific output vectors, or classify input vectors in an appropriate way as defined by you. Networks with biases, a sigmoid layer, and a linear output layer are capable of approximating any function with a finite number of discontinuities. Properly trained Backpropagation networks tend to give reasonable answers when presented with inputs that they have never seen. Typically, a new input leads to an output similar to the correct output for input vectors used in training that are similar to the new input being presented. This generalization property makes it possible to train a network on a representative set of input/target pairs and get good results without training the network on all possible input/output pairs. There are generally four steps in the training process:

- Assemble the training data
- Create the network object
- Train the network
- Simulate the network response to new inputs

4.2. Fuzzy Logic

Fuzzy logic has rapidly become one of the most successful of today's technologies for developing sophisticated control systems. The reason for which is very simple. Fuzzy logic addresses such applications perfectly, as it resembles human

decision making with an ability to generate precise solutions from certain or approximate information. It fills an important gap in engineering design methods left vacant by purely mathematical approaches (e.g. linear control design), and purely logic-based approaches (e.g. expert systems) in system design. . In general meaning, *Fuzzy logic* is a super-set of conventional (Boolean) logic that has been extended to handle the concept of partial truth- truth values between "completely true" and "completely false".

As its name suggests, it is the logic underlying modes of reasoning which are approximate rather than exact. The importance of fuzzy logic derives from the fact that most modes of human reasoning and especially common sense reasoning are approximate in nature.

To understand the reasons for the growing use of fuzzy logic it is necessary, first, to clarify what is meant by fuzzy logic. In a narrow sense, fuzzy logic is a logical system, which is an extension of multivalued logic. But in a wider sense, which is in predominant use today, fuzzy logic (FL) is almost synonymous with the theory of fuzzy sets, a theory that relates to classes of objects with unsharp boundaries in which membership is a matter of degree. In this perspective, fuzzy logic in its narrow sense is a branch of FL. What is important to recognize is that, even in its narrow sense, the agenda of fuzzy logic is very different both in spirit and substance from the agendas of traditional multivalued logical systems.

4.2.1. Background

The precision of mathematics owes its success in large part to the efforts of Aristotle and the philosophers who preceded him. In their efforts to devise a concise theory of logic, and later mathematics, the so-called "Laws of Thought" were posited. One of these, the "Law of the Excluded Middle," states that every proposition must either be True or False. Even when Parminedes proposed the first version of this law (around 400 B.C.) there were strong and immediate objections: for example, Heraclitus proposed that things could be simultaneously “True and not True”.

It was Plato who laid the foundation for what would become fuzzy logic, indicating that there was a third region (beyond True and False) where these opposites "tumbled about."

In the early 1900's, Lukasiewicz described a three-valued logic, along with the mathematics to accompany it. The third value he proposed can best be translated as the term "possible" and he assigned it a numeric value between True and False. Eventually, he proposed an entire notation and axiomatic system from which he hoped to derive modern mathematics. Later, he explored four-valued logics, five-valued logics, and then declared that in principle there was nothing to prevent the derivation of an infinite-valued logic. Lukasiewicz felt that three-and-infinite-valued logics were the most intriguing, but he ultimately settled on a four-valued logic because it seemed to be the most easily adaptable to Aristotlean logic.

Knuth proposed a three-valued logic similar to Lukasiewicz's, from which he speculated that mathematics would become even more elegant than in traditional Šbi-valued logic. His insight, apparently missed by Lukasiewicz, was to use the integral range [-1, 0 +1] rather than [0, 1, 2]. Nonetheless, this alternative failed to gain acceptance, and has passed into relative obscurity.

It was not until relatively recently that the notion of an infinite-valued logic took hold. In 1965, Lotfi A. Zadeh published his seminal work "Fuzzy Sets" which described the mathematics of fuzzy set theory, and by extension fuzzy logic. This theory proposed making the membership function (or the values False and True) operate over the range of real numbers [0.0, 1.0]. New operations for the calculus of logic were proposed, and showed to be in principle at least a generalization of classic logic. It is this theory which we will now discuss.

The first applications of fuzzy theory were primarily industrial, such as process control for cement kilns. However, as the technology was further embraced, fuzzy logic was used in more useful applications. Fuzzy logic was also put to work in elevators to reduce waiting time. Today, the applications range from consumer products such as cameras, camcorders, washing machines, and microwave ovens to industrial process control, medical instrumentation, decision-support systems, and portfolio selection.

4.2.2. Fundamentals of Fuzzy Sets

Fuzzy logic comprises of concepts like fuzzy sets, membership functions, basic set operations, complement etc.

4.2.2.1. Fuzzy set

Professor Lofti Zadeh at the University of California formalized fuzzy Set Theory in 1965. What Zadeh proposed is very much a paradigm shift that first gained acceptance in the Far East and its successful application has ensured its adoption around the world.

A paradigm is a set of rules and regulations, which defines boundaries and tells us what to do to be successful in solving problems within these boundaries. For example the use of transistors instead of vacuum tubes is a paradigm shift - likewise the development of Fuzzy Set Theory from conventional bivalent set theory is a paradigm shift. A *fuzzy set* is a set without a crisp, clearly defined boundary. It can contain elements with only a partial degree of membership between 0 and 1.
A classical set might be expressed as;

$$A = \{x \mid x > 6\} \qquad \text{Eqn. 4.7}$$

A fuzzy set is an extension of a classical set. If X is the universe of discourse and its elements are denoted by *x*, then a fuzzy set A in X is defined as a set of ordered pairs.

$$A = \{x, \mu A(x) \mid x \in X\} \qquad \text{Eqn. 4.8}$$

$\mu A(x)$ is called the membership function (or MF) of *x* in A. The membership function maps each element of X to a membership value between 0 and 1.

For better understand what a fuzzy set is, first consider what is meant by what we might call a *classical set*. A classical set is a container that wholly includes or wholly excludes any given element. According classical set, *of any subject, one thing must be either asserted or denied.* For example, the set of degree of room temperature unquestionably includes cold, cool, warm and hot. It just as unquestionably excludes sun, fly, and so on.

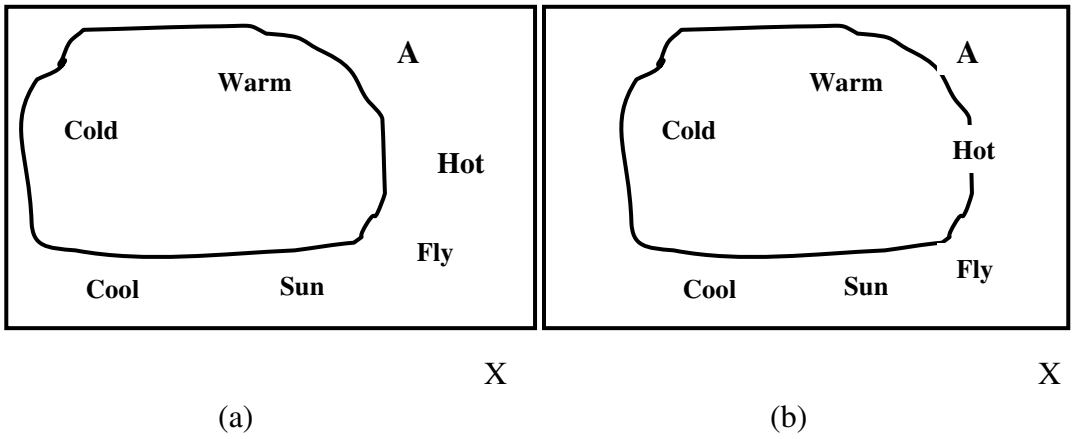

(a) (b)

Figure 4.4. (a) Elements in Classical set A, (b) Fuzzy set A (A: Room Temperature, X: Universe)

In classical set, there is a sharp boundary. The set excludes the term "hot" out of room temperature. However, fuzzy set includes the term "hot" as a matter of degree of room temperature. T*he truth of any statement becomes a matter of degree.*

4.2.2.2. Membership function

A membership function (MF) is a curve that defines how each point in the input space is mapped to a membership value (or degree of membership) between 0 and 1. The input space is sometimes referred to as the universe of discourse (X), a fancy name for a simple concept. The curve or line is often given the designation of μ.

There are many various kinds of membership functions. The simplest membership functions are formed using straight lines. Of these, the simplest is the *triangular* membership function. It is nothing more than a collection of three points forming a triangle. The *trapezoidal* membership function, trapmf, has a flat top and really is just a truncated triangle curve. These straight-line membership functions have the advantage of simplicity. Two membership functions are built on the *Gaussian* distribution curve: a simple Gaussian curve and a two-sided composite of two different Gaussian curves. The *generalized bell* membership function is specified by three parameters and has the function name gbellmf. The bell membership function has one Foundations of Fuzzy Logic more parameter than the Gaussian membership function, so it can approach a non-fuzzy set if the free parameter is tuned. Because of their

smoothness and concise notation, Gaussian and bell membership functions are popular methods for specifying fuzzy sets. Both of these curves have the advantage of being smooth and nonzero at all points. Polynomial based curves account for several of the membership functions in the toolbox. Three related membership functions are the *Z, S*, and *Pi curves*, all named because of their shape. The function zmf is the asymmetrical polynomial curve open to the left, smf is the mirror-image function that opens to the right, and pimf is zero on both extremes with a rise in the middle.

4.2.2.3. Basic Fuzzy Set Operations

The most important thing to realize about fuzzy logical reasoning is the fact that it is a superset of standard Boolean logic. In other words, if we keep the fuzzy values at their extremes of 1 (completely true), and 0 (completely false), standard logical operations will hold.

The membership function of the Union of two fuzzy sets A and B with membership functions μ_A and μ_B and respectively is defined as the maximum of the two individual membership functions. This is called the *maximum* criterion. The Union operation in Fuzzy set theory is the equivalent of the **OR** operation in Boolean algebra. Then, basic relations for fuzzy sets are defined. The operator is denoted as:

$$\mu_{A\cup B} = \max(\mu_A, \mu_B) \qquad \text{Eqn. 4.9}$$

The membership function of the Intersection of two fuzzy sets A and B with membership functions μ_A and μ_B respectively is defined as the minimum of the two individual membership functions. This is called the *minimum* criterion. The Intersection operation in Fuzzy set theory is the equivalent of the **AND** operation in Boolean algebra.

$$\mu_{A\cap B} = \min(\mu_A, \mu_B) \qquad \text{Eqn. 4.10}$$

The membership function of the Complement of a Fuzzy set A with membership function; μ_A^- is defined as the negation of the specified membership function. This is

called the *negation* criterion. The Complement operation in Fuzzy set theory is the equivalent of the **NOT** operation in Boolean algebra.

$$\mu_{\bar{A}} = 1 - \mu_A \qquad \text{Eqn. 4.11}$$

4.2.3. Fundamentals of Fuzzy Logic

Human beings make decisions based on rules. Although, we may not be aware of it, all the decisions we make are all based on computer like if-then statements. If the weather is fine, then we may decide to go out. If the forecast says the weather will be bad today, but fine tomorrow, then we make a decision not to go today, and postpone it till tomorrow. Rules associate ideas and relate one event to another. Fuzzy machines, which always tend to mimic the behavior of man, work the same way. However, the decision and the means of choosing that decision are replaced by fuzzy sets and the rules are replaced by fuzzy rules. Fuzzy rules also operate using a series of if-then statements. For instance, if X then A, if y then b, where A and B are all sets of X and Y. Fuzzy rules define fuzzy *patches*, which is the key idea in fuzzy logic.

A machine is made smarter using a concept designed by Bart Kosko called the Fuzzy Approximation Theorem (FAT). The FAT theorem generally states a finite number of patches can cover a curve as seen in the Figure 4.5. If the patches are large, then the rules are sloppy. If the patches are small then the rules are fine.

Figure 4.5. Fuzzy Patches

In a fuzzy system this simply means that all our rules can be seen as patches and the input and output of the machine can be associated together using these patches.

Graphically, if the *rule patches* shrink, our fuzzy subset triangles get narrower. Naturally, it is *math-free* system.

4.2.4. Fuzzy systems

To create a fuzzy system, four components are needed. They are fuzzification, fuzzy rule base, fuzzy output engine, and defuzzification. A general fuzzy system is exhibited in Figure 4.6.

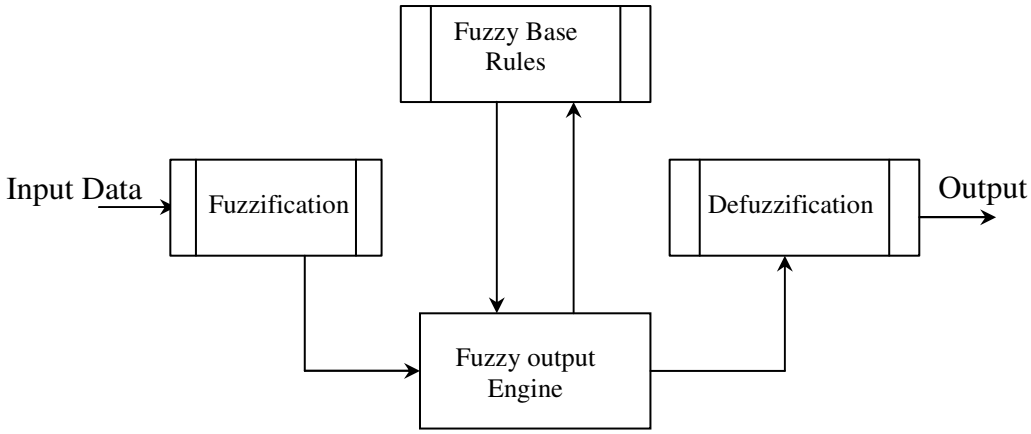

Figure 4.6. Steps of fuzzy logic approach.

4.2.4.1. Fuzzification

Under *Fuzzification,* the membership functions defined on the input variables are applied to their actual values, to determine the degree of truth for each rule premise. A membership function (MF) is a curve that defines how each point in the universe of discourse is mapped to a value between 0 and 1. Intuitions, inference, rank ordering, angular fuzzy sets, neural networks, genetic algorithms, and inductive reasoning can be among many ways to assign membership values for functions to fuzzy variables.

4.2.4.2. Fuzzy Inference Engine

Fuzzy inference is the actual process of mapping from a given input to an output using fuzzy logic. Fuzzy inference engine uses the knowledge of fuzzy rules to learn how to transform a set of inputs to corresponding output. There are two kinds of inference operator: minimization (min) and product (max). They can be written in terms of membership functions as:

$$\mu B(y) = MAX\ [MIN(\mu_A(x), \mu_R(x,y))]\ x \in E1 \qquad \text{Eqn. 4.12}$$

$$\mu B(y) = MAX\ [\mu_A(x)\ .\ \mu_R(x,y)]\ x \in E1 \qquad \text{Eqn. 4.13}$$

where Eqn. 4.12 is for min and Eqn. 4.13 is for prod operators.

4.2.4.3. Defuzzification

The input for the *defuzzification process* is a fuzzy set (the aggregate output fuzzy set) and the output is a single number-crispness recovered from fuzziness at last. As much as fuzziness helps the rule evaluation during the intermediate steps, the final output for each variable is generally a single crisp number. So, given a fuzzy set that encompasses a range of output values, we need to return one number, thereby moving from a fuzzy set to a crisp output. There are many defuzzification methods (Zadeh): bisector of area, centre of area, means of maxima, leftmost maximum and rightmost maximum. In this study, we employed the most commonly used centroid method and bisector of area. It was thought that there was no considerable change in the modeling performance results.

For a discrete universe of discourse, the defuzzified output is defined as;

$$u^* = \frac{\sum_{i=1}^{N} u_i \mu_{OUT}(u_i)}{\sum_{i=1}^{N} \mu_{OUT}(u_i)} \qquad \text{Eqn. 4.14}$$

where u^* is defuzzified output value, u_i is the output value in the i^{th} subset, and $\mu(u_i)$ is the membership value of the output value in the i^{th} subset. For the continuous case, the summation terms in Eqn.4.14 are replaced by integrals.

CHAPTER 5

CEMENT MILLING PROCESS

5.1. Cement Milling Process

Cement milling process applied in the local plant is a closed circuit system with a tube mill and a mechanical air separator (Figure 5.1).

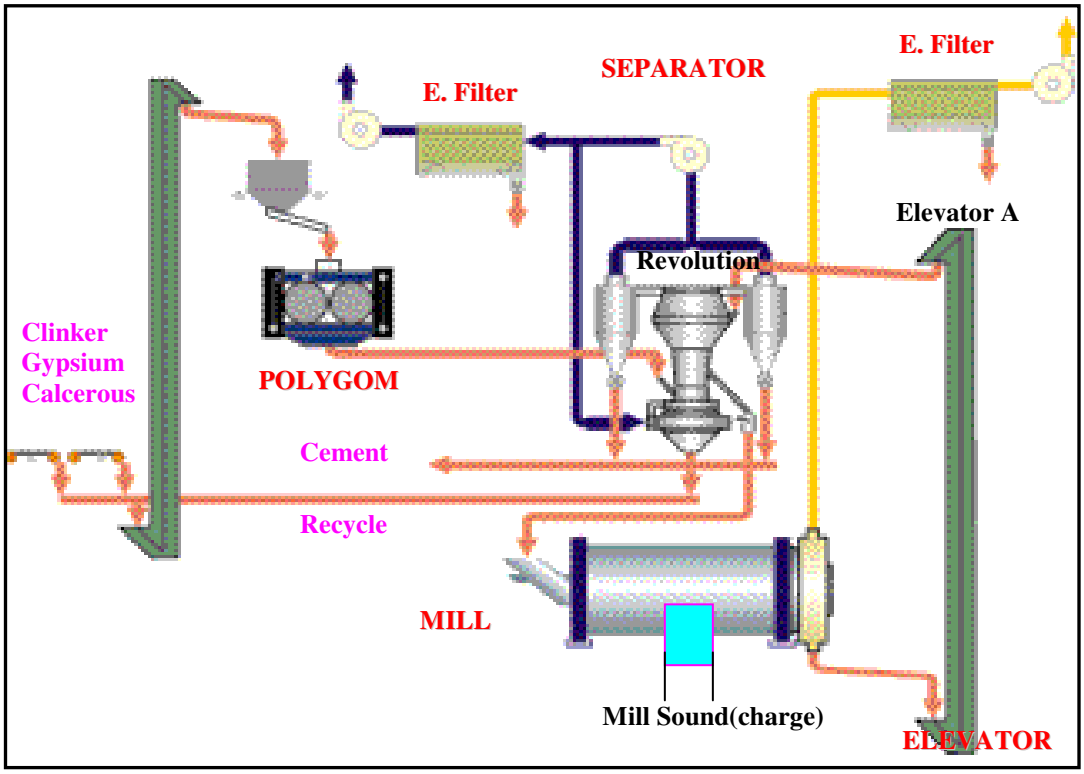

Figure 5.1. Closed-Circuit Cement Milling process.
(Source: CEMBERNAU 1996)

The process is consists of three stages: feeding, grinding, and separating.

5.1.1. Feeding

Portland cement is produced by inter-grinding clinker with a few percent of natural or industrial gypsum or anhydrite (calcium sulphate) acting as a set regulator. In many European countries, the addition of up to 5% of "minor constituents" such as raw meal, limestone or filter dust is allowed.

The clinker, which is transported from the clinker storage, is pre-ground by Polycom®, which is a pre-grinding system with Roller Press. The ground clinker is mixed with additive materials (gypsum and calcareous) in a main belt conveyor after weighted by weighting machine.

5.1.2. Grinding

The mill, which is a tube type mill, has a dimension of 15 m x 5.5 m. It is horizontally rotating steel cylinder, where size reduction of the mill feed is performed by motion of the grinding media. It consists of three compartments: drying compartment, pre-milling compartment and final milling compartment (Figure B.3).

The capacity of the mill is 220 t/h. The feed charge to the mill varies between 150 t/h and 220 t/h according the cement type. For portland cement production the feed of clinker and additive material is 170 ± 10 t/h. The critical speed of a mill is that speed of rotation at which the centrifugal power neutralizes the force of gravity, which influence the grinding balls. The rotational speed of the mill varies between 14 and 15 rpm according ball charge in the mill. The flow of material in the mill is provided by the help of vacuum created by a fan.

In the drying compartment, the fresh feed (clinker, gypsum or calcareous) and recycled feed into the tube mill is dried by the help of hot gas coming from the kilns. In addition to drying, homogenous mixing of clinker and additive materials is provided by steel mixing spoons.

In the pre-milling compartment, there are steel balls of a radius of 70, 80 and 90 mm. They reduce the size of the mixed feed particles to be ground more efficiently. To provide homogenous milling, there are some shell liners constructed on the inside shell. These liners also prevent the different sized balls to move forward to the end of the room and mix each other. To prevent passing of oversized particles to the next

compartment, there is a sieve diaphragm with double wall. The finer particles pass through a sieve diaphragm with slots to the final milling compartment.

In the final milling compartment, smaller balls of radius of 30, 40, 50 and 60 mm exist. The smaller voids between the balls provide effective milling of mixed material. As in the pre-milling compartment, there are liners constructed on the inside-shell for homogeneous mixing and certain placement of different sized balls. At the end, there is a sieve diaphragm with single wall for effective milling. The finer particles, which pass through the slots, are sent to the separator by the help of a bucket-elevator.

5.1.3. Separation

Separation as performed by mechanical air separators is the division of a given material stream into two separate streams, using air as the carrying medium. The separation is performed by a Polysius Cyclone Air Separator® in the plant (Figure B.4).

The material is introduced laterally into the separator by an air-slide, and it is uniformly distributed in the separating chamber by the distribution plate. An externally mounted blower produces the air stream, which flows through the material in the separating zone classifying the material into course and fine particles by the effect of gravity and the air current. The fines particles entrained in the air current are participated in the cyclones, which are equipped with air seals. The dust-free air is returned to the blower and re-enters the separator through adjustable rings of guide vanes. The incoming air flows through the coarse particles as they trickle down over series of buffles, thus exerting a secondary separation effect. The fineness of the finished product can be regulated over wide range during operation of the separator by changing, predominantly, the speed (rotation) of the distributed plates

5.2. Parameters Affecting On Fineness

The cement milling process has many parameters affecting on the fineness. We can classify these parameters into three parts: mechanical, chemical-physical parameters and operational parameters.

5.2.1. Mechanical Parameters

The mechanical parameters are related with the mill and separator dimensions and physical characteristics such as length and radius of mill, ball sizes, and radius of slots over sieve diaphragm etc. Since there is no change in these parameters during operation, we can accept that these parameters are constant.

5.2.2. Chemical-Physical Parameters

These parameters include clinker and additive material contents. Chemical content of clinker (C_3S, C_2S) affects mineralogical structure of clinker; hence, grindibility of the clinker. Grindibility has an important role in the cement milling process. However, it is difficult to sustain grindibility tests in continuous milling system.

5.2.3. Operational Parameters

They are parameters, which are adjusted to get efficient operational conditions and better fineness. In the local plant, cement milling process is performed by the help of many operational parameters. However, some of parameters are vital to control the process. They are *falofon*, *elevator amperage* and *revolution*. All of these factors have varying degrees of effect on fineness of the milled product which is either measured as weight percentage of product residue on 32-μm sieve or as Blaine (surface area per unit of milled product, cm^2/g).

5.2.3.1. Revolution Level

The material transported to the separator is divided into two streams: fine and course particles. The separation is performed by the control of centrifugal and gravitational force balance. By changing the revolution level (%) (Instant rotational speed x 100 / max rotational speed), centrifugal force can be controlled; hence, the fineness and finished product weight can be adjusted in the separator (Figure 5.1).

5.2.3.2. Falofon® Level

Usually, best grinding occurs when the mill is most noisy, indicative of many grinding actions taking place within the mill. The falofon level, which is function of mill noise, reflects the percentage ratio of instant media and feed charge to max media and feed charge (Figure 5.1). Falofon® level is usually measured as a process control parameter to monitor mill operation.

5.2.3.3. Elevator Amperage Level

The ground material is transported to the separator by an elevator for being divided into a flow of rejected oversized particles, which are returned to the mill inlet to be reground, and a flow of fine particles, which forms the final product (Figure 5.1). Hence, the amount of material in the elevator to be sent to the separator can be measured as a function of the amperage level of the elevator motor.

CHAPTER 6

MODEL CONSTRUCTION

Data collected from Çimentaş for a period of one year (2004) were employed in this thesis. Two combined modelling studies were performed using this data:

1) The ANN model with 3 parameters on MatLAB®
2) The fuzzy model on MatLAB®

The response surface of the ANN model was then used for determining the rule set of the Fuzzy Model. Such procedure is used by Tagaki and Hayashi (Tagaki – Hayashi Method) in 1990.

6.1. Data Collection

The data collected from the local plant that uses 32-μm sieve fineness test for process control. The data belong to the period between the months of January and December 2004. All the mechanical and operational parameters are controlled and observed by online system. The operators observe the process by the help of computers and decide the future process trends.

On the other hand, there is no online control for cement analysis. Cement sample is collected by the help of screw-sampling instrument during operation. An operator assistant takes cement sample to the laboratory in every hour.

Sieve analysis is carried out by Alpine Machine® according EN standard (EN 196-6). The machine consists of from the sieves containing different sized holes. 100 g of cement sample is used for the analysis. The fineness of cement is measured by sieving it on standard sieves. The proportion of cement of which the grain sizes are larger than the specified size is thus determined (EN 196-6). The result is recorded as percentage (%) by weight.

6.2. Data Reduction

The cement milling operation in the local plant can be performed different types of cement (CEM II/A-W 42.5 R, CEM II/A-P-W 42.5 R, CEM II/B-P-W 42.5 R and CEM I 42.5 R). Hence, the data of portland cement (CEM I 42.5 R) was chosen after elimination of the other cement types' operational and quality parameters.

The process mechanical defects (vibration of engine, plate defects, etc.) and operational faults (plugging of mill and air system, software false alarms, etc.) create gaps in the data. Therefore, these defected data were eliminated before construction of the model.

Furthermore, the process includes many operational parameters (feed flow-rate, entrance and existence temperature of the mill, air flow-rate of hot gases, etc.) to control the system. Most of them are related each other. For example, the feed rate and void of material in the mill can be controlled by falofon; Air flow-rate to the separation unit can be also interrelated with revolution of distribution plates. The amount of output material from the mill tube to the separator can be also observed by elevator amperage.

Finally, we got three input parameters (Revolution, Falofon and Elevator Amperage) and one output parameter (32-μm fineness, %wt). The 155 data points for three inputs and one output parameter used in the modelling are given in Tables A.1. The input and output variables descriptive statistics of the data are tabulated in Table 6.1.

Table 6.1. Statistics of input and output variables used in model construction.

Code	Input variable	Descriptive statistics of the data		
		Min	Average	Max
$\tilde{x}_1$	Rotational speed (%)	63	65.2	68
$\tilde{x}_2$	Falofon (%)	92	93.8	96
$\tilde{x}_3$	Elevator Amps	66	77.2	99
y	Fineness, wt % (32-μm sieve)	14.0	16.3	18.7

6.3. Modelling

6.3.1. ANN Model

In this study, the common three-layer feed-forward type of ANN, as shown in Figure 6.1 was considered.

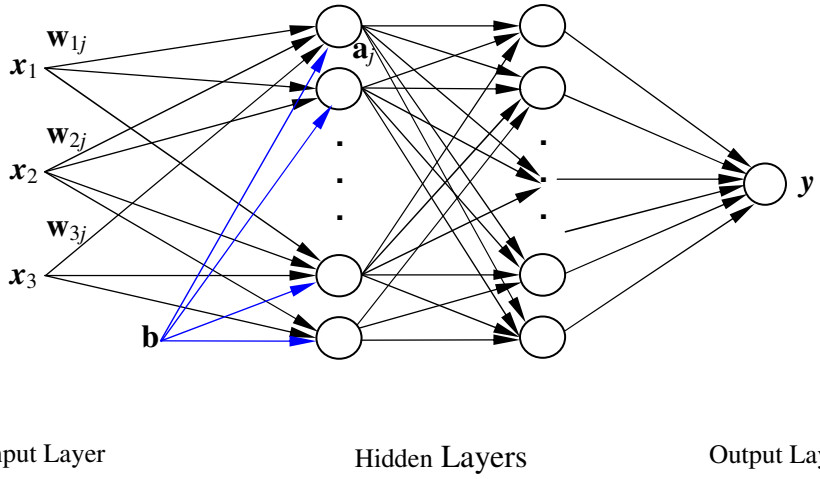

Figure 6.1. **A** typical back-propagation ANN model.

In the feed forward network, the data of input parameters are to be normalized using before feeding into input layer. Input layer passes them on to the hidden layer neurons after multiplying by weight matrix. Then, the weighted input is added up by the hidden layer and associated with a bias. The result is passed through a nonlinear function. The operation is repeated by output layer.

The values of weights change between -1 and 1, randomly. The network is first trained. Adjusting the weights and biases through some training algorithm minimizes the error, which is the difference between the target output and the calculated model output at each output neuron. In this study, tangent sigmoidal function (Eqn.6.1) was employed as an activation function in the training of the network.

$$f(u_i) = \tan sig(u_i) \qquad \text{Eqn.6.1}$$

The learning of ANNs is accomplished by a backpropagation algorithm where information is processed in the forward direction from the input layer to the hidden layers and then to the output layer (Fig. 6.1). The objective is to minimize error term described by Eqn.7.2 for finding optimal network weights that would generate an output vector Y = (y_1) as close as possible to target values of output vector T = (t_1) without compromising prediction accuracy over new data-set. Error function has the following form [10]:

$$E = \sum_{p} \sum_{m} (y_i - t_i)^2 \qquad \text{Eqn.6.2}$$

where y_i is the component of an ANN output vector Y, t_i is the component of a target output vector T, *m* is the number of observations of the output; and *p* is the number of training patterns.

In this study, the ANN architecture was of feed-forward type composed of four layers (Fig. 6.1). There were 3 neurons in the input layer for the 3 input variables. Each of the two hidden layers had 10 neurons. In the output layer, one neuron was used for the output variable of cement fineness. The last version of the model architecture, which gave the best result, was reached after trial of many model variations.

There were a total of 155 observations collected from the year 2004. The data set was randomly splitted into two parts: the first part was used for training (120 data points) and the second part (35 data points) for testing of the model (Table A.2). Computer algorithm for the neural network written in MATLAB® was run for 5000 batches with 1000 iterations at each batch. At each batch, new network weights and biases were calculated. This was done to allow the search for optimal network that minimizes the error associated with testing data.

6.3.2. Fuzzy Logic Model

Creation of the fuzzy model of the milling system is exhibited in Figure 6.2. Each membership function for inputs and outputs was created in MatLAB® fuzzy logic toolbox. Mamdani rules were defined, and Min method was chosen for fuzzy inference engine. In defuzzification part of the model, in order to obtain defuzzified results, COG (centroid) method was applied.

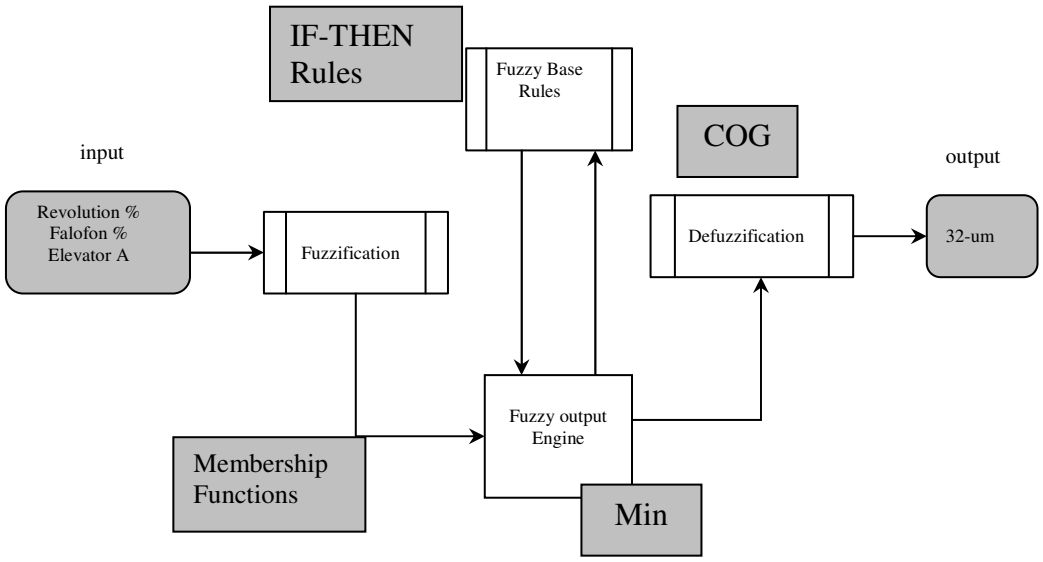

Figure 6.2. Fuzzy Model of Portland Cement Milling in Tube-Ball Mill on MatLAB®.

6.3.2.1. Rule Creation by Means of Response Surface Obtained Via ANN Model

Fuzzy logic rules are verbal expressions in "IF-THEN" format like IF Revolution is low AND elevator A is medium THEN fineness is high. To create rules partial sensitivity analysis was performed by feeding input parameters, falofon and revolution, at varying levels of elevator amperage into the developed model and prediction outputs of cement fineness. The whole range of input parameter, elevator amperage, was divided into three parts to have continuous plot for factor effects. In order to make partial sensitivity analysis with two parameters (revolution and falofon), one parameter, elevator amperage, was held constant at the mean values of level ranges. These ranges and means are tabulated in Table 6.2.

Table 6.2. Ranges and Means of Elevator A used in the rule creation.

Elevator Amp.	Ranges	Means
Low	66-72	69
Medium	72-82	78
High	82-96	87

After running sensitivity analysis on the created ANN model, response contour plots were made using the input parameters (Revolution-, Falofon, and Elevator amps) and the output (fineness) parameter (Figure 6.3 to Figure 6.5).

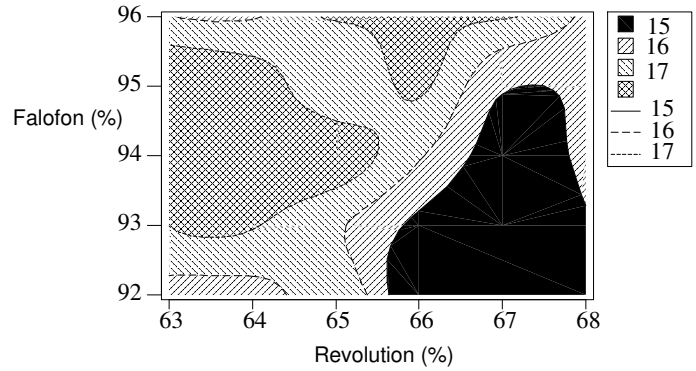

Figure 6.3. The response contour plot of the ANN model at Elevator Amps: 69.

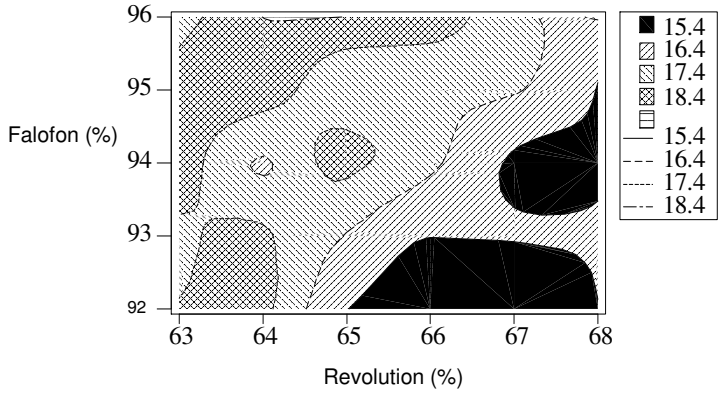

Figure 6.4. The response contour plot of the ANN model at Elevator Amps: 78.

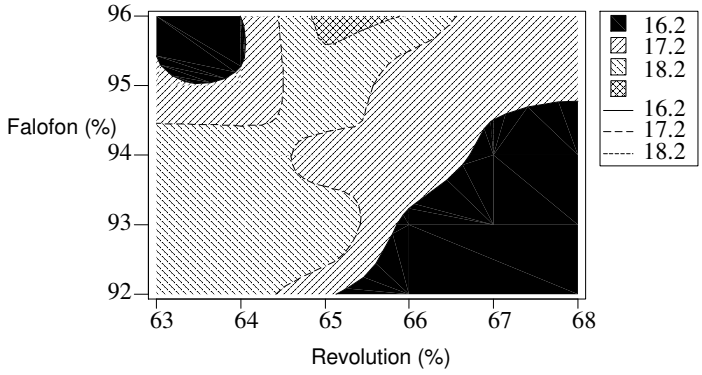

Figure 6.5. The response contour plot of the ANN model at Elevator Amps: 87.

In the plots, the region labeled with 15-16 % wt is low for fineness. 16-17 % wt is exhibited as medium for fineness. Finally, the region 17-18 % is shown as high for fineness.

For low values (Figure 6.3), and at low revolution (%) as falofon increases, the fineness makes a positive curve. The curve reaches its highest value when falofon is medium about 94 %. For medium revolution values, increasing falofon level increases the fineness. For high degree of revolution and low degree of falofon, fineness is mainly low. Increasing the falofon level increases the fineness % to the medium level

For medium amperage values (Figure 6.4) and at low revolution level (%) as falofon increases, the fineness is predominantly high. For medium revolution values, increasing falofon level increases the fineness. For high degree of revolution and low degree of falofon, fineness makes S shape behavior. First, fineness increases as falofon increases. At the medium level of falofon, it decreases to low level. Finally, it increases to medium level at the high level of falofon.

For high amperage values (Figure 6.5) and at low revolution level (%) as falofon increases, the fineness is mainly medium. At the highest level of falofon, fineness decreases to low degree. For medium revolution values, increasing falofon level increases the fineness from low degree to high degree. For high degree of revolution and low degree of falofon, fineness is predominantly low. At high degrees of falofon, it reaches medium level.

By detailed analysis of values of parameters of ANN model's contour plots, the fuzzy rules are created. There is three parameters and three levels, then there will be 3^3 (27) rules for the fuzzy model. This 27 fuzzy rule-set is listed in Table 6.3. In this study, High level is labeled as "H"; medium level is exhibited as "M", and finally, low level is labeled as "L".

Table 6.3. Mamdani-type fuzzy rule sets (27 rule-set).

Input Parameters			Output Parameter
Revolution %	**Falofon %**	**Elevator A**	**32 um (% weight)**
L	L	L	M
L	L	M	H
L	L	H	M
L	M	L	H
L	M	M	H
L	M	H	H
L	H	L	H
L	H	M	H
L	H	H	H
M	L	L	L
M	L	M	L
M	L	H	M
M	M	L	M
M	M	M	M
M	M	H	H
M	H	L	M
M	H	M	H
M	H	H	H
H	L	L	L
H	L	M	L
H	L	H	M
H	M	L	L
H	M	M	M
H	M	H	M
H	H	L	M
H	H	M	M
H	H	H	M

(L: Low; M: Medium; H: High)

6.3.2.2. Membership Functions

In this study, four membership functions (Mf's) were created: three for input parameters and one for the output. The numbers of subsets were selected for each mf using the range for each parameter (Table 6.1). Fuzzy Mf's may be formed in *triangular, trapezoidal* or *Gaussian sigmoidal geometries.* In this study, we constructed mix of *Z-mf, S-mf* and *gaussmf* membership functions of the input parameters and response. This mix of Mf's was called as Z-S-gaussmf. The membership functions of revolution and fineness are exhibited in Figure 6.6.

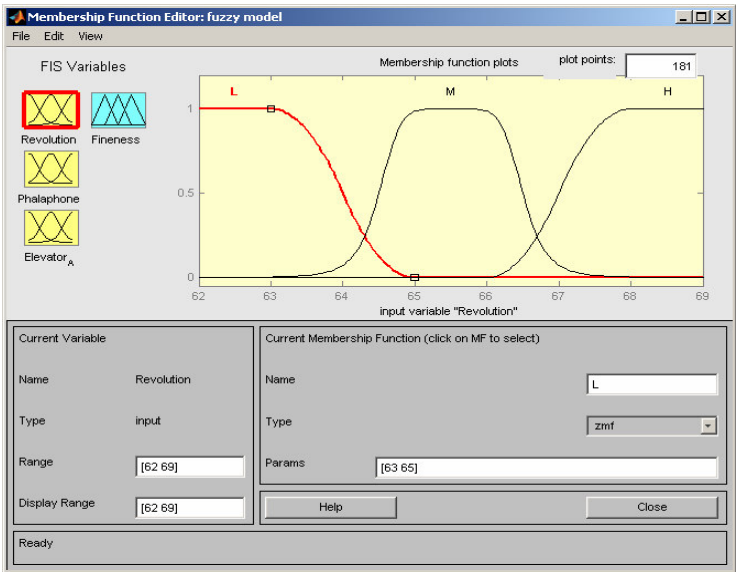

(a)

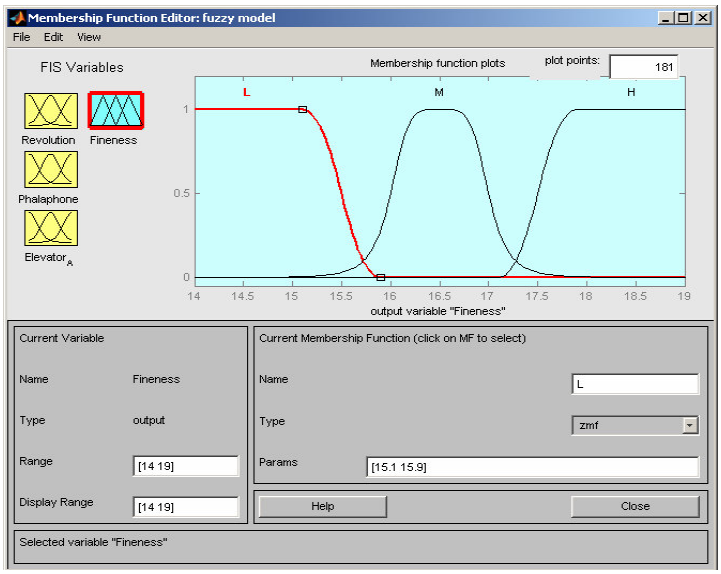

(b)

Figure 6.6. (a) Mf for Revolution and (b) Mf for Fineness used for fuzzy modelling.

The membership functions of falofon (%) and Elevator Amperage (A) are shown in Figure B.5 and Figure B.6.

The Mamdani-type rule set that has been created by the help of response surface area of ANN model result is coded in MatLAB® fuzzy rule editor. IF-THEN sentences and “and” operator are used to construct the rule set.

6.3.2.3. Testing of the Fuzzy Logic Model

The 35 sets of input data (Table A.2) were fed into the model and as a result, 35 sets defuzzified output values were obtained from the model. These were predicted 32-μm cement fineness values, which were then compared with actual 35 sets 32-μm cement fineness values.

CHAPTER 7

RESULT AND DISCUSSION

In this study, the ANN architecture was of feed-forward type composed of four layers (Figure 6.1). 155 observations (Table A.1) collected from the year 2004 were collected to construct ANN-Fuzzy model. The dataset was randomly divided into two parts: the first part (120 data points) was used in order to train the model, and the second part (35 data points) for testing of the model. Computer algorithm for the neural network written in MatLAB® was run for 5000 batches with 1000 iterations at each batch.

At each batch, new network weights and biases were calculated. This was done to allow the search for optimal network that minimizes the error associated with testing data. The network having the best R^2 was saved.

In Figure 7.1, comparison of actual and predicted values for 32-µm Fineness, % wt, for training of the model is exhibited.

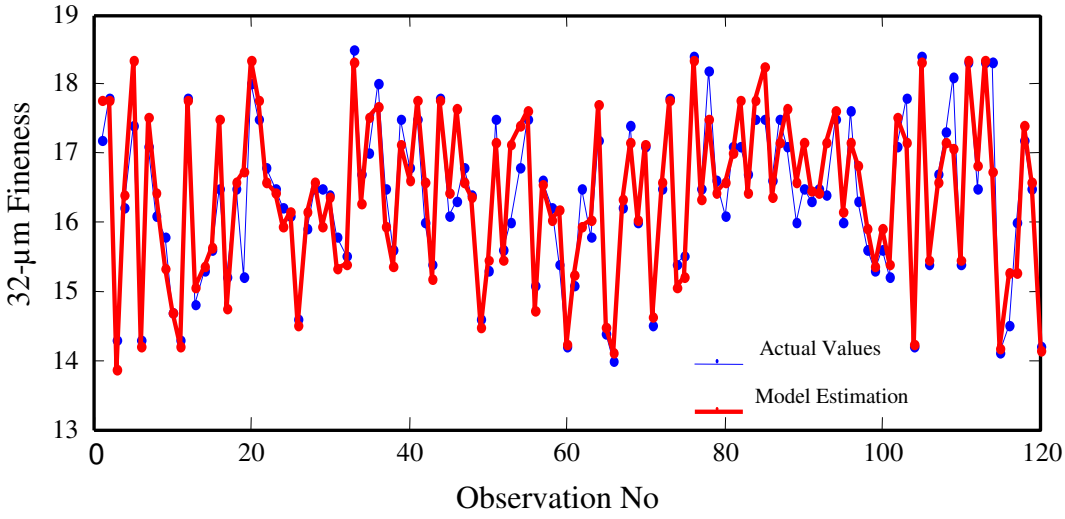

Figure 7.1. Actual and predicted values for 32-µm Fineness, % wt (Training).

It is observed that the model estimation followed the actual value of the data on most of points. Only small deviations from the actual values for 32-µm fineness can be seen.

Figure 7.2 plots the residuals versus the fitted values for 32-µm fineness, % wt. Obviously, most of residuals (more than 80 %) fall within the limits ±1 and are scattered around the mean, "0", without negative or positive tendency. Also, there is no potential outlier in the plot.

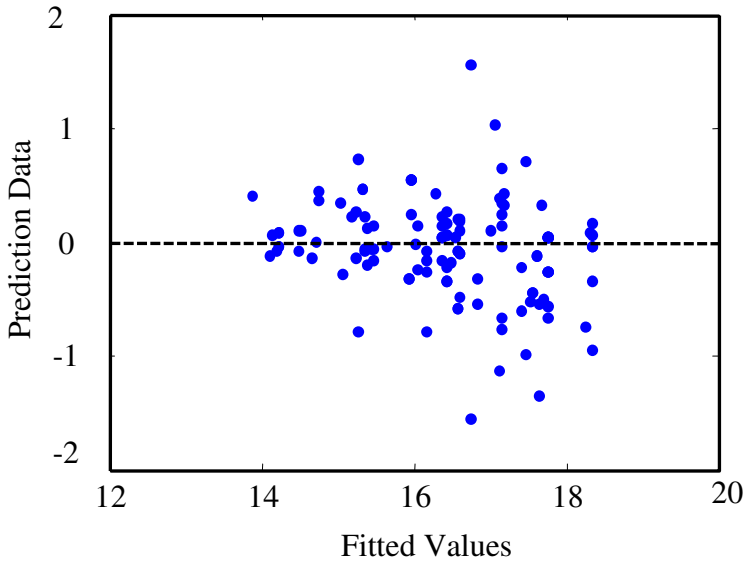

Figure 7.2. Residuals versus fitted values (Training).

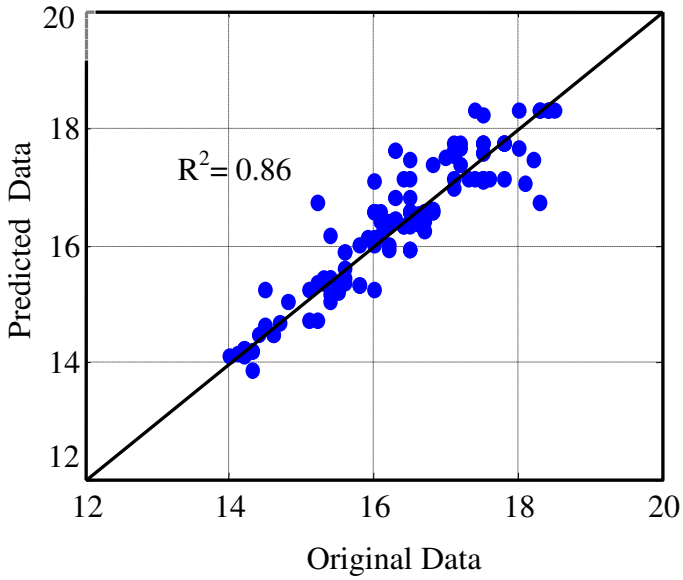

Figure 7.3. Prediction performance plot (Training).

Therefore, the result reflected on prediction performance plot with a correlation coefficient of 0.93 (Figure 7.3).

The trained model was tested by comparing it to actual measured data that formed a group of 35 observations (Table A2) from the same year.

Although a few model predicted values (15th, 21st and 28th observations) deviate from the actual observed values, most of the model values followed the actual observed values of fineness (Figure 7.4).

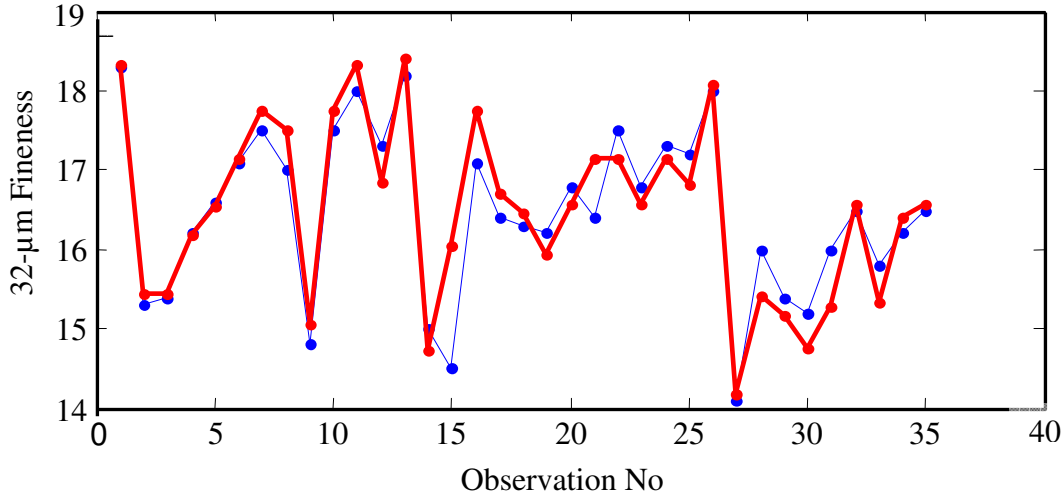

Figure 7.4. Observed and predicted values for 32 µm Fineness, % (Testing).

Except 15th observation, the distribution in the residuals versus fitted values plot of testing (Figure 7.5) got narrower than the residuals versus fitted values plot of the training part.

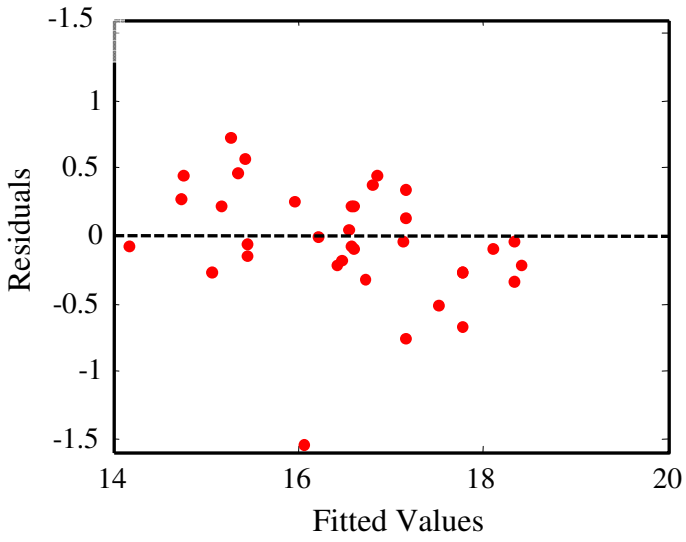

Figure 7.5. Residuals versus Fitted values (Testing).

In Figure 7.6, testing prediction performance of the model is presented. Clearly, the model's ability to predict the 32-µm fineness was good giving an R^2=0.85.

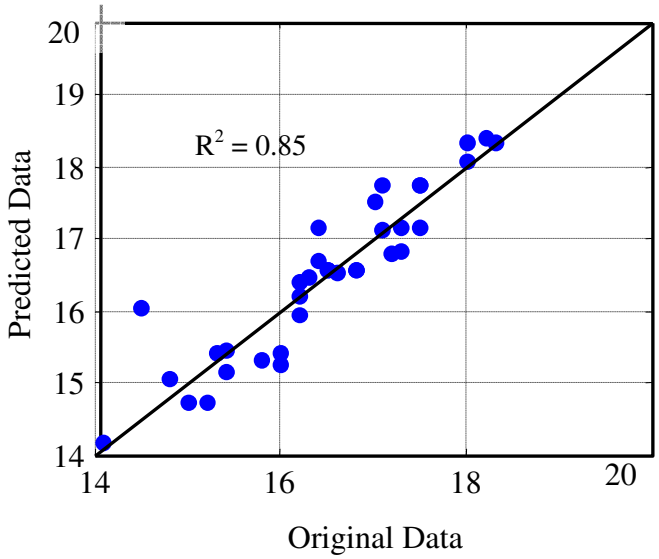

Figure 7.6. Prediction performance plot (Testing).

After running sensitivity analysis on the created model, response contour plots were made using the input parameters (rotational speed, falofon, and elevator amp.), and the output parameter (fineness) at different degrees of Elevator Amperage (Low, Medium and High). The figures (Figure 6.3, Figure 6.4, and Figure 6.5) were exhibited in Chapter 6.

According the operational conditions, 15-16 % wt fineness region was exhibited as low. Similarly, 16-17 % wt and 17-18 % is wt fineness region were labeled for medium and high values of fineness, respectively.

In Figure 6.3, it was observed that the fineness make a positive curve at low revolution (%) as falofon increases when elevator amperage was kept low degree. Frankly, the curve reaches its highest value when falofon is medium about 94 %. Furthermore, an increase in the fineness is seen when falofon value is increased at medium revolution values. In addition to this, fineness ranges between low values for high degree of revolution and low degree of falofon. . Increasing the falofon level increases the fineness % to the medium level.

In Figure 6.4, it was realized that fineness ranges between high values as falofon increases at low values of revolution level (%) for medium amperage values. For medium revolution values, increasing falofon level increases the fineness. In addition to this result, an S-shaped tendency in fineness is seen clearly when revolution is high and falofon is low. First, fineness increases as falofon increases. At the medium level of falofon, it decreases to low level. Finally, it increases to medium level at the high level of falofon.

In Figure 6.5, it was observed that fineness the fineness is mainly medium as falofon increases at low revolution level (%), when elevator amperage is kept at high values. The scene changes that fineness decreases to low degree at the highest level of falofon. However, increasing falofon level increases the fineness from low degree to high degree for medium revolution values. For high degree of revolution and low degree of falofon, fineness is predominantly low. At high degrees of falofon, it reaches medium level.

The response surface, which was constructed by the help of the ANN model prediction, was then used for determining the rule set of the Fuzzy Model. The procedure, which used to construct the Fuzzy model, contains formation of membership functions of parameters, creation of Mamdani-type rule set, fuzzy output engine and defuzzification. Detailed information about the model construction is given in Chapter 6.

Fuzzy Viewer, an output of the Fuzzy Logic Toolbox of MatLAB®, is easy to exhibit the fineness value by changing input parameters (Revolution %, Falofon % and Elevator A) in the input blank below the scheme. By using the Fuzzy Viewer, user is able to view which degrees of parameters are used.

The developed fuzzy logic-based model was applied to predict 35 sets of 32-µm Fineness, % wt (Table A.2). The actual 32-µm fineness, % wt, (35 test data) was compared with the predicted 32-µm fineness, % wt, in Figure 7.7.

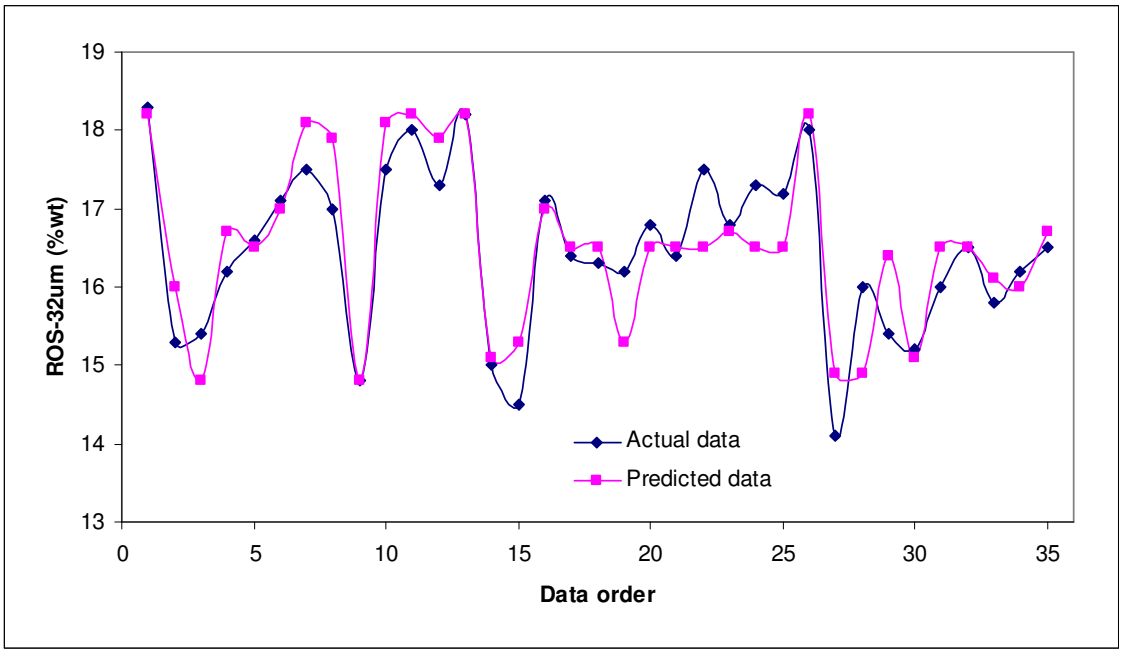

Figure 7.7. Observed and predicted values for 32 µm Fineness (% wt).

As seen from Figure 7.7, the predicted 32-µm fineness, % wt, values followed the actual 32-µm fineness, % wt, values with small errors, expect a few points.

Absolute average percent error (AAPE) of the model was calculated by following equation:

$$AAPE = \frac{1}{N}\sum \frac{|obs.fineness - pred.fineness|}{obs.fineness} \times 100\% \qquad \text{Eqn. 7.1.}$$

A brief statistics of the fuzzy logic-based model is exhibited in Table 7.1.

As a result of error calculation of the model, it was realized that the models gave a minimum error of 0 % and maximum error of 6.875 %. Finally, AAPE of the model was 2.764 %, which showed that the performance of the model was very good.

Table 7.1. Statistics of Fuzzy model Errors

Statistics	Error
Min	0
Max	6.875
AAPE	2.764
Std. Dev	2.161

In Figure 7.8, the actual fineness values of the process and predicted fineness of the created fuzzy logic-approach model was plotted.

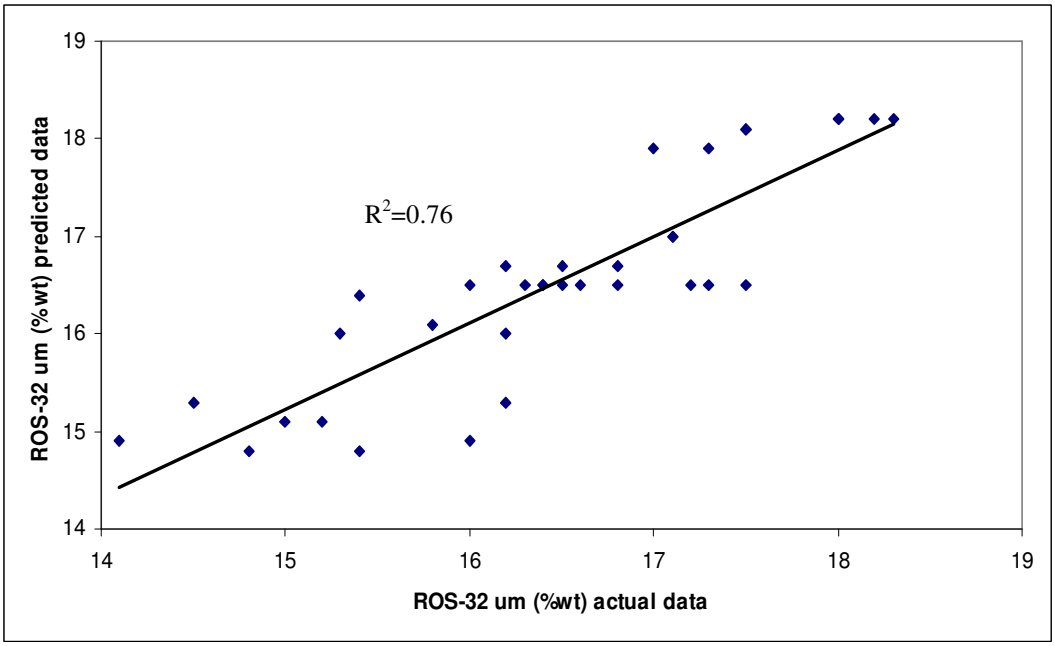

Figure 7.8. Actual Fineness versus predicted fineness values of the Fuzzy Model.

It was realized that the model had an R^2=0.76. About 24 % of the total variation could not be accounted for. This can be explained by the other cement milling parameters such as grindibility of clinker, inlet temperature of the mill inside and deformation of the balls.

CHAPTER 8

STATISTICAL MONITORING OF CEMENT FINENESS

Portland cement is produced by burning of a solid mixture of limestone and clay in a rotary kiln at a temperature of 1300 to 1500 ^{o}C, and grinding of this material with a few percent of gypsum (up to 5 %) in a cement mill to a very fine powder. Cement milling process is a closed system. The process, basically, consists of three stages: feeding, milling and separation. Coarse raw material is ground by a tube mill, and fine particles are separated by a separator. Quality of cement, mostly, is resembled by mortar compressive strength. Chemical structure, fineness and particle size distribution of finished product have a strong influence on mortar compressive strength. Due to this reason, cement sample produced in the process is analyzed in every hour. Among these parameters, product residue on 32-μm sieve, %wt, (fineness) has greatest importance on monitoring of the process. Any shift in this parameter indicates problem on the process conditions.

In order to monitor 32-μm fineness, %wt, of cement, the local plant applies basic Individual Control Chart. However, it has been observed that the chart does not correspond small shifts. If the high production rate (180 ± 10 ton / h) is considered, these shifts may lead problems with the cement stocked in the silos with capacity of 10.000 t.

In this study, in addition to I-MR control chart, CUSUM, EWMA and Moving Average (MA) control charts were applied in order to detect small shifts. The performances of these control charts are to be compared. As software, MINITAB® was used to construct statistical monitoring.

8.1. Measurement

The cement milling process is very sensitive that all parameters on the system are to be monitored by great care. Each machine in the system is automatically controlled and measured. The process operators observe the process by the help of computers and decide future process trends.

However, there is no online control for cement analysis. An operator assistant sends cement sample, which is collected by a sampling instrument near the cement silos, in every hour, to the laboratory. Chemical structure, Blaine and 32-µm sieve (%wt) and 90-µm sieve (% wt) analyses are applied according to EN standards.

32-µm (%wt) analysis is carried out by Alpine Machine® according EN 196-6 standard. It consists of from the sieves containing different sized holes. 100 g of cement sample is used for sieve analysis. As the machine vacuums the material, the fine material passes through the holes. The material that cannot pass through the holes is weighted. The weight percent of residue on sieve gives fineness of the cement.

8.2. Data Collection

The data used in statistical monitoring were collected from a local cement plant that uses 32-µm sieve analysis for process control. The data are shown in Table 8.1 and Table 8.2. Phase I includes the data when the process is in-control. Phase II data is a normal process data to be monitored.

Table 8.1. Base Data of 32-µm (%wt) fineness of the Cement Type PC-42.5 (Phase I).

Obs. no	***Fineness (%wt)***	***Obs. no***	***Fineness (%wt)***	***Obs. no***	***Fineness (%wt)***
1	15.5	*11*	17.1	*21*	16.3
2	17.7	*12*	16.5	*22*	16
3	17.7	*13*	16.1	*23*	16.6
4	15.1	*14*	20.2	*24*	16.5
5	16.7	*15*	18.1	*25*	17.1
6	16.8	*16*	16.7	*26*	16
7	16.4	*17*	16.1	*27*	18.7
8	18.4	*18*	18.6	*28*	17.1
9	17.8	*19*	16.7	*29*	15.6
10	17.5	*20*	16.4	*30*	16.1

Table 8.2. Monitoring Data of 32-μm fineness of the Cement Type PC-42.5 (Phase II).

Obs. no	*Fineness (%wt)*	*Obs. no*	*Fineness (%wt)*	*Obs. no*	*Fineness (%wt)*
1	17.4	*22*	17.6	*43*	17.5
2	16.1	*23*	16.7	*44*	16.9
3	17.6	*24*	17.3	*45*	16.8
4	16.6	*25*	18.4	*46*	17.4
5	16.8	*26*	18	*47*	17.5
6	17.4	*27*	17.4	*48*	16.9
7	15.9	*28*	18.8	*49*	17.2
8	16.5	*29*	16.6	*50*	17.6
9	18.5	*30*	17.5	*51*	17.9
10	16	*31*	17.1	*52*	18.5
11	18.3	*32*	17.2	*53*	17.6
12	16.2	*33*	15.6	*54*	17.3
13	16.8	*34*	18	*55*	18
14	16.1	*35*	16.5	*56*	18.4
15	16.1	*36*	16.9	*57*	17.7
16	16.3	*37*	15	*58*	17.6
17	17.3	*38*	16.1	*59*	17.8
18	18	*39*	18.6	*60*	18.5
19	18.3	*40*	17.5	*61*	17.7
20	17.5	*41*	16.6	*62*	17.8
21	15.6	*42*	18.5	*63*	17.7

8.3. Checking Correlation and Normality of the Process Data

8.3.1. Correlation Check

In this step, we have to check whether there is any correlation (or time dependency) in the data. If any correlation is determined in the data, we have to eliminate this correlation to use the standard control charts. Autocorrelation analysis of

the data is to be applied so that ant time dependency of the 32-µm (%wt) fineness data can be seen. Figure 8.1 exhibits the autocorrelation function of the data.

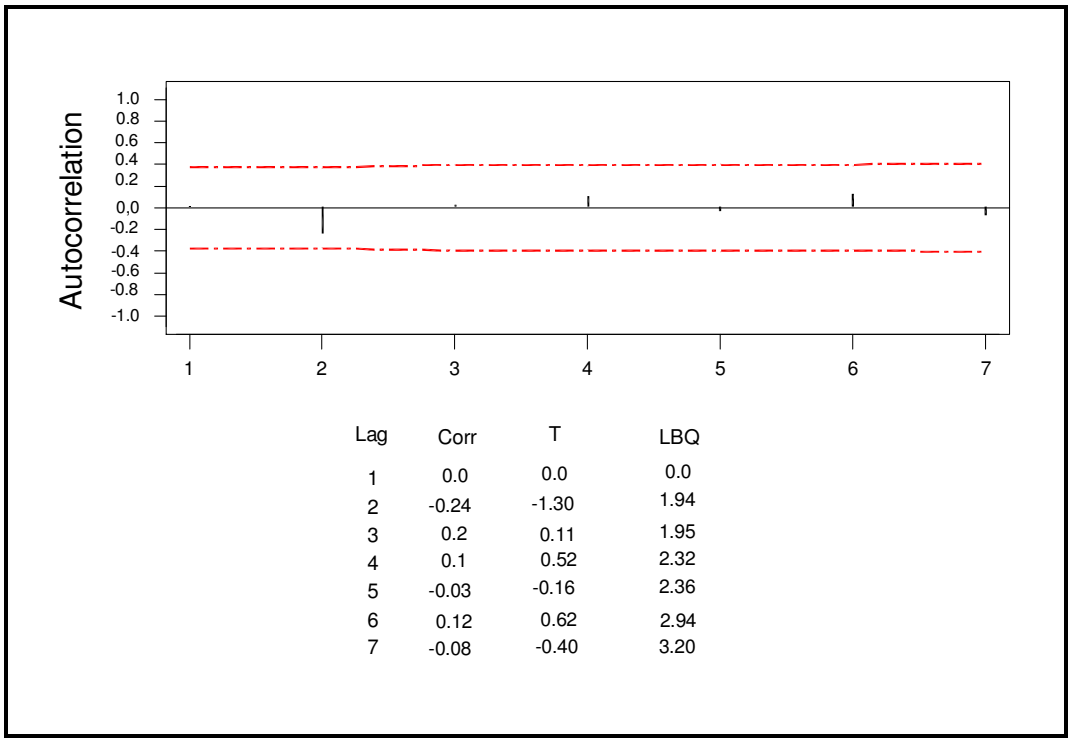

Lag	Corr	T	LBQ
1	0.0	0.0	0.0
2	-0.24	-1.30	1.94
3	0.2	0.11	1.95
4	0.1	0.52	2.32
5	-0.03	-0.16	2.36
6	0.12	0.62	2.94
7	-0.08	-0.40	3.20

Figure 8.1. Autocorrelation function for 32-µm (%wt) fineness data (Phase I).

Obviously, there is no evidence that there is an autocorrelation in the data, since no sample autocorrelation do not exceeds its standard deviation limit. And also, corresponding autocorrelation parameter ρ_k is likely zero. Figure 8.2 supports this result that there is any tendency (positive or negative) between data at time t and the data at time t-1.

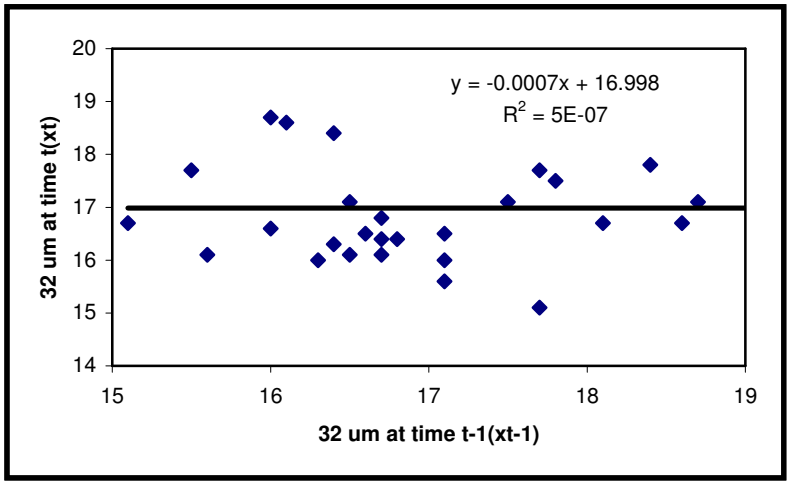

Figure 8.2. Scatter plot of 32-µm fineness at time t (x_t) versus 32-µm fineness one period earlier (x_{t-1}).

8.3.2. Normality Check

In order to determine whether there exists a departure from the normality, normal probability plot of the data (phase I) is plotted in 95 % confidence interval (Figure 8.3). The mean and standard deviation of the data is estimated by *Least Linear Square method* and found to be 16.936 and 1.092 respectively. To determine goodness of fit, *Anderson-Darling statistic* and *Pearson correlation coefficient* are calculated. The Anderson-Darling statistic is (AD) a measure of how far the plot points fall from the fitted line in a probability plot. MINITAB® uses an adjusted Anderson-Darling statistic, in which points in the tails are weighted more. A smaller Anderson-Darling statistic indicates that the distribution fits the data better. In this study, AD is found to be 0.997, which is small.

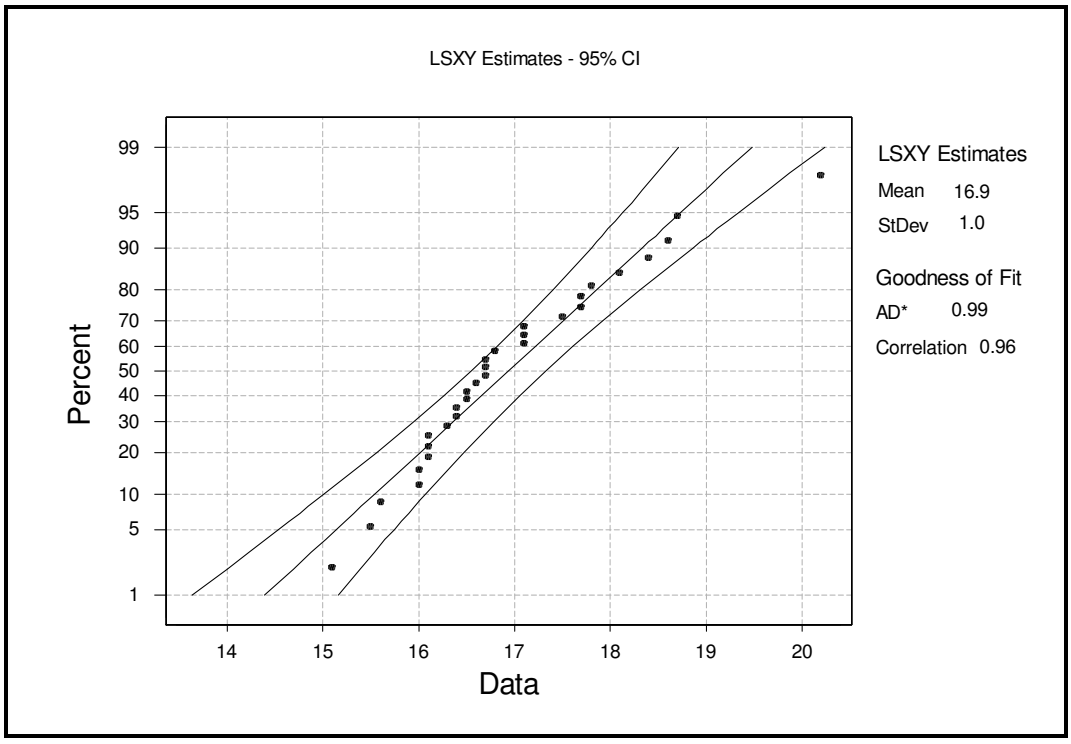

Figure 8.3. Normal Probability Plot of the 32-μm fineness data (Phase I).

For Least Squares Estimation, MINITAB® calculates a *Pearson correlation coefficient*. If the distribution fits the data well, then the plot points will fall on a straight line. The correlation measures the strength of the linear relationship between the X and Y variables. The correlation will range between 0 and 1, and higher values indicate a better fitting distribution. In this study, the correlation coefficient is found to be 0.966. This result is not very good that the data shows some departure from the normality. This can be easily seen from the figure that the last point creates this departure. It is to be eliminated in the control charts in order to monitor future process data in a clear way.

8.4. Monitoring 32-μm Fineness (%wt) of Cement

In this section, the best control chart type is to be found for 32-μm fineness (%wt) monitoring. In cement grinding process, one cement sample is taken every hour (n=1); that the sample consists of an individual unit. The Shewhart control charts for means and ranges are not usually applicable. In this situation, I-MR, CUSUM and EWMA control charts are applied for process monitoring.

8.4.1. Establishing Trial Control Limits

Any out of control point is to be identified and eliminated before historical data (Phase I) is used for future process data (Phase II). To detect whether any out of control point existed in the historical data, I-MR Chart, Figure 8.4, is used.

As seen from the figure, there is an out of control point (14th observation). The point, obviously, exceeds three-sigma limit (UCL) of both graphs. The time of this point is found in the charts and it is found that the Polycom®, which is a pre-milling machine of the system, had been stopped as a result of vibration in its rollers. This problem causes the raw material to be ground insufficiently.

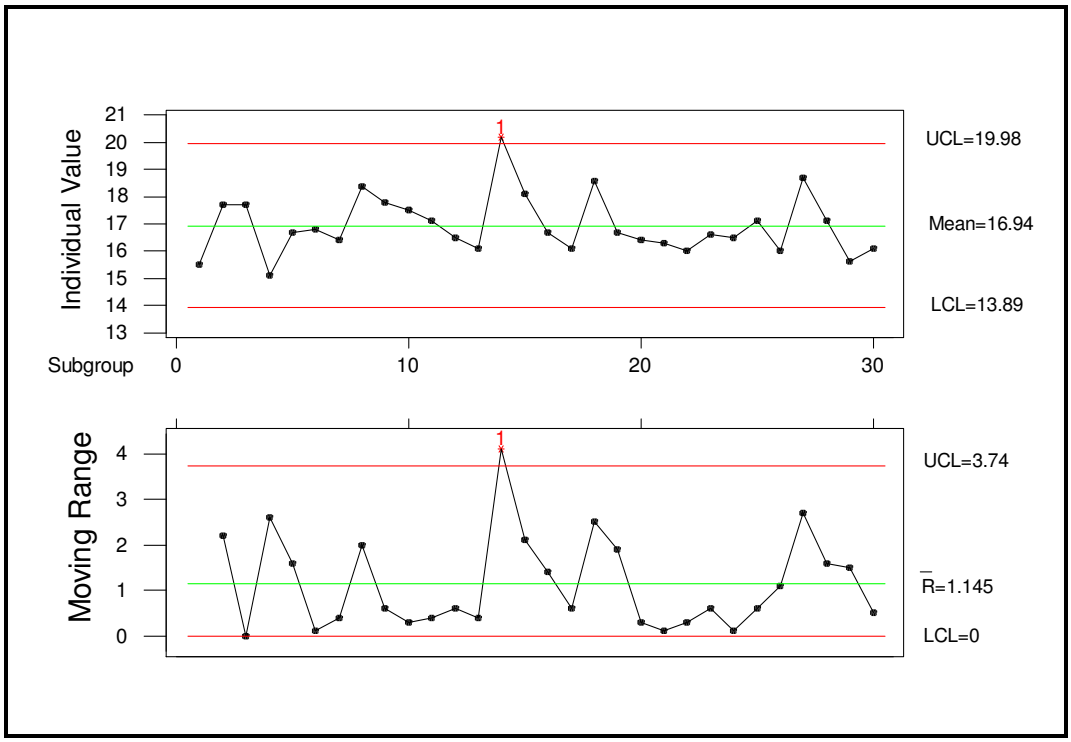

Figure 8.4. I-MR Chart for the historical 32-µm (%wt) fineness Data (Phase I).

The point is to be eliminated and a new I-MR chart is constructed for new control limits (Figure 8.5).

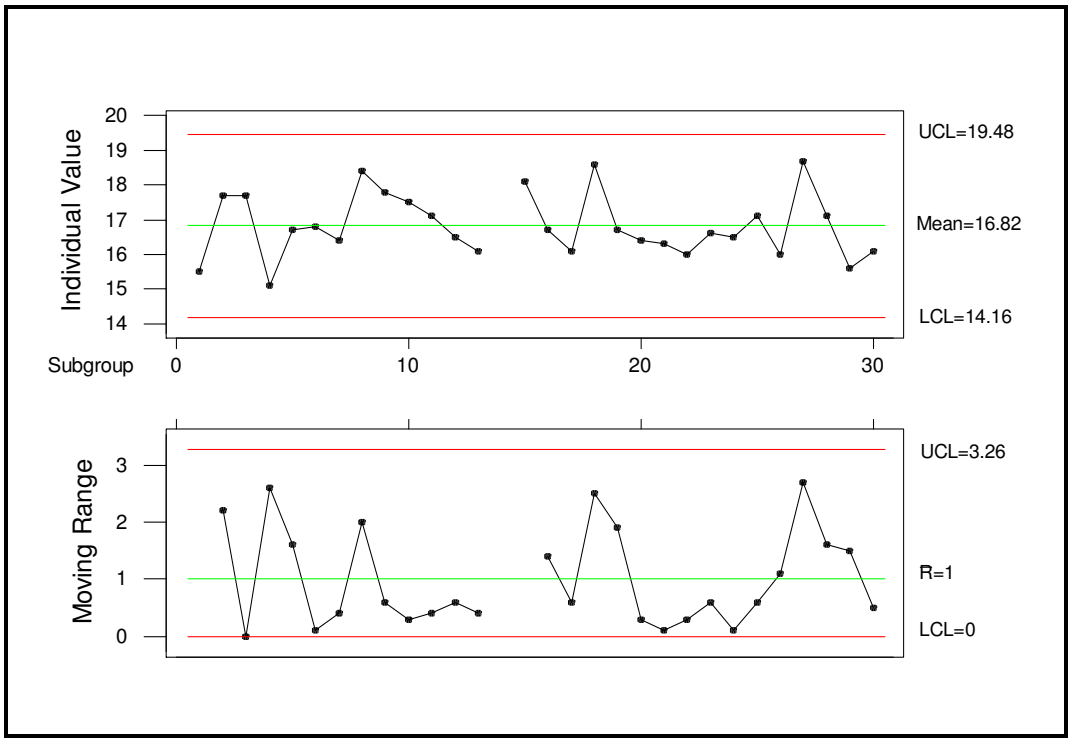

Figure 8.5. I-MR Chart for the Phase I data after elimination of out of control point.

The new I-MR plot indicates no out of control point so we can use new control limits and mean in future process data (Phase II). The effect of elimination of out of control point can be seen on the Normal probability plot of the data (Figure 8.6). The new AD is decreased to 0.804 and Pearson correlation is increased to 0.994. There seems no departure from the normality.

8.4.2. Process Capability Analysis for Phase I

In order to justify the results for any risk, process capability analysis is applied the data after elimination of the out of control point (Figure 8.7). In the process, upper and lower specification limits are 19.5 and 14, respectively. It is seen that the data follow a normal distribution and $C_p \cong C_{pk} = 1.03$, which shows that process fall out approximately 16.82 % wt.

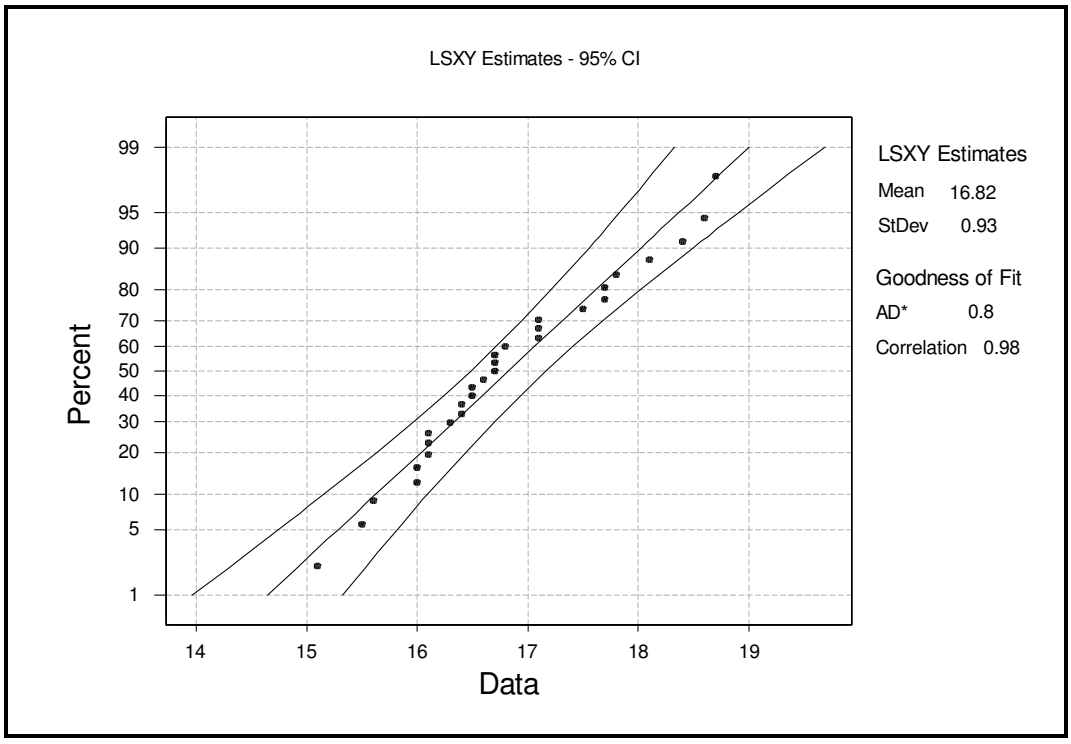

Figure 8.6. Normal Probability Plot of the Phase I data after elimination of out of control point.

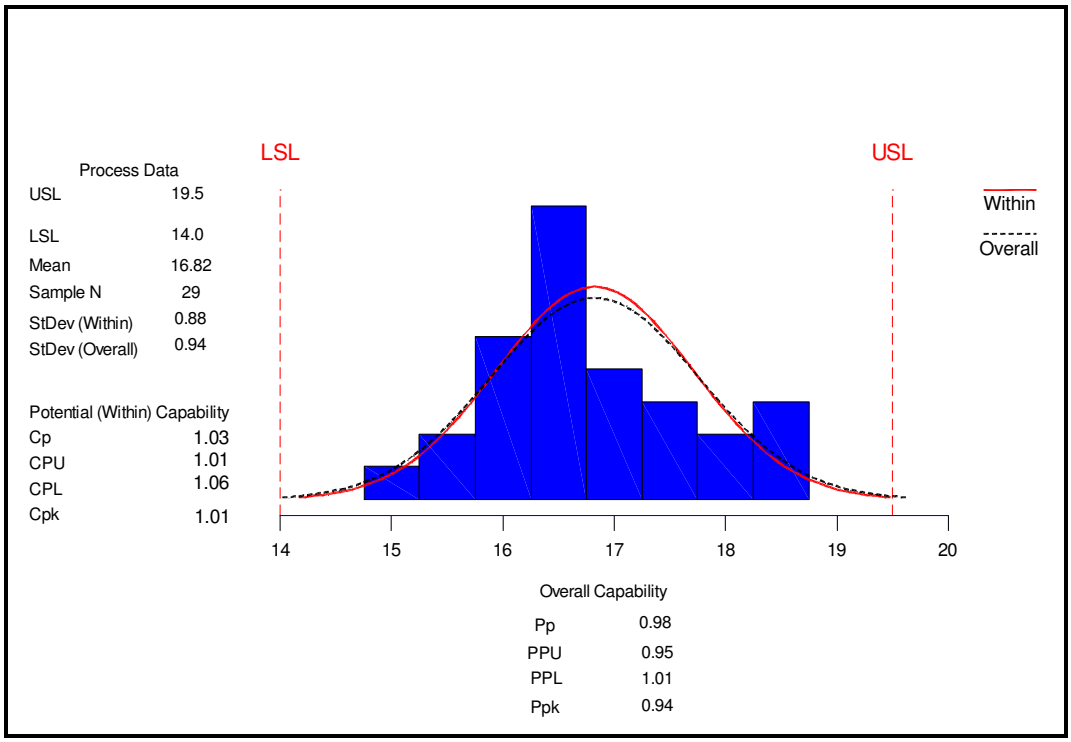

Figure 8.7. Process capability analysis for eliminated Phase I data.

8.5. Statistical monitoring of the future data (Phase II)

In Table 8.2, the future process data is given. To detect if there exists shift in the process mean, I-MR chart, CUSUM and EWMA Control charts are constructed.

8.5.1. I-MR Control Chart

The MR chart is applied to the process data by using historical data control limits, mean and standard deviation (Figure 8.8).

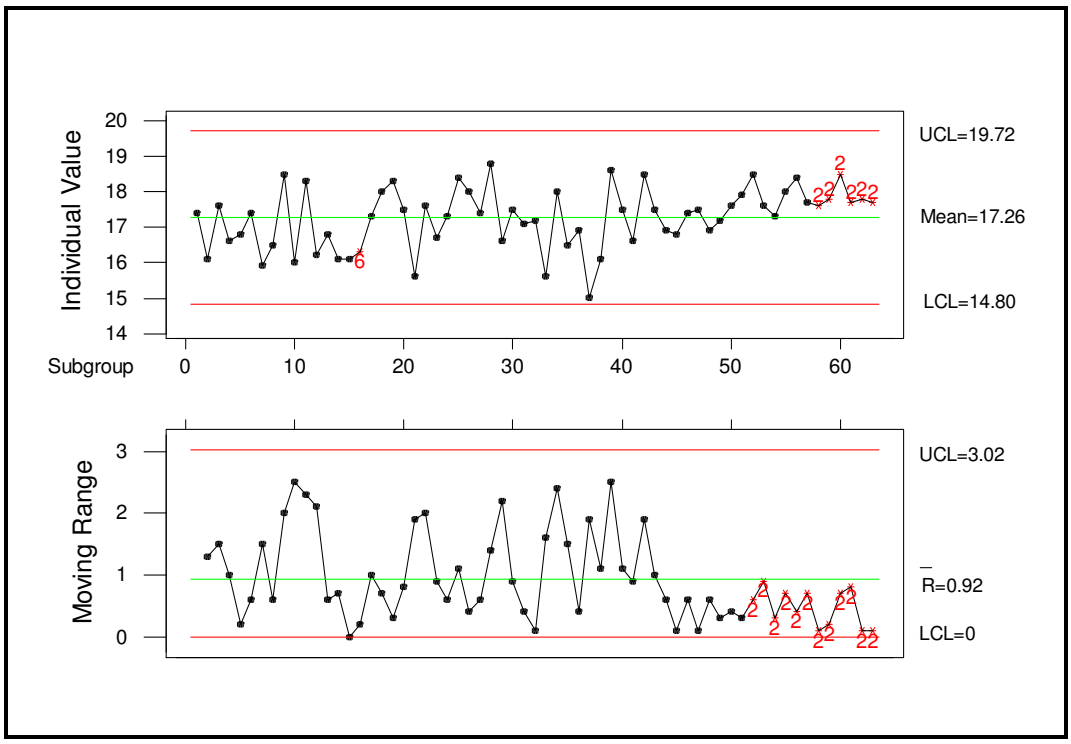

Figure 8.8. I-MR Chart for the Phase II data.

As illustrated in Figure 8.8, points in a row on same side of centerline of I-chart. The same points (52, 53, 54, 55, 56, 57, 58, 59, 60, 61, 62, and 63) are seen on the MR chart. Moreover, 4 out of 5 points more than 1 sigma from centerline (on one side of CL) of the I-chart. Test fails at 16th observation. Although all the sensitizing rules are applied, detecting this shift may be difficult in the process. It may not give any alarm of out of control. It is clear that the ability of the I-MR chart to detect small shift is very poor.

8.5.2. CUSUM Control Chart

Since the small shift could not be detected by I-MR chart, CUSUM control chart, Figure 8.9, is applied to the process data (Phase II). As target value, 16.8 % wt of 32-μm fineness is selected. h and k values are taken as 4 and 0.5, respectively.

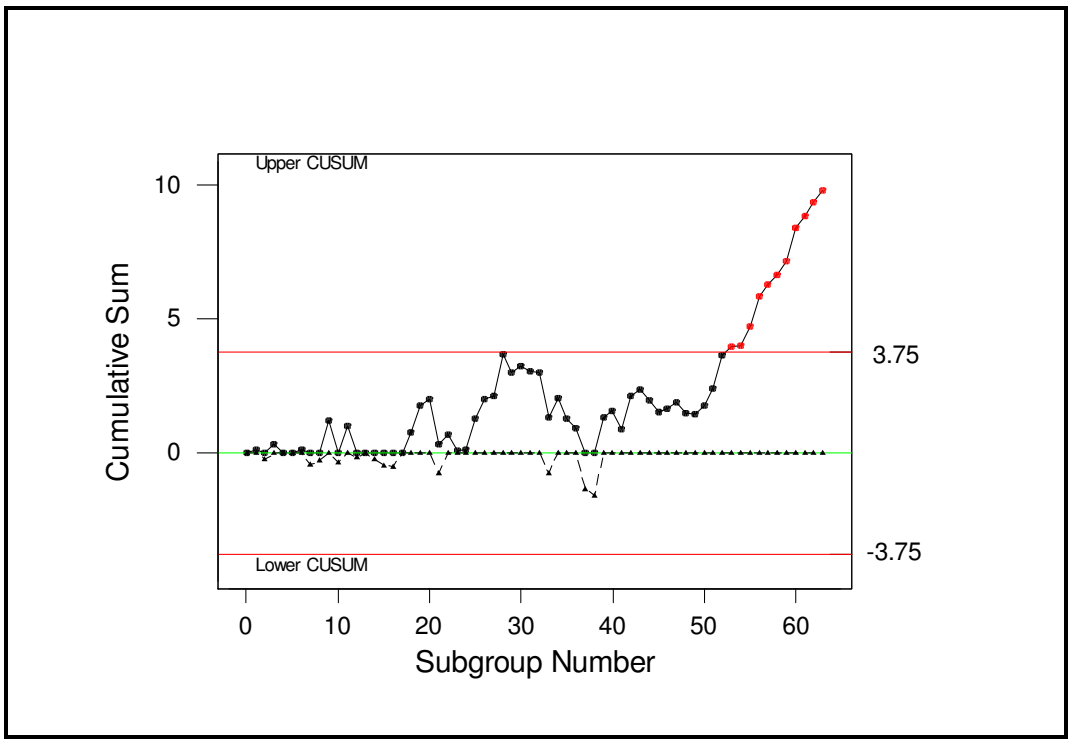

Figure 8.9. CUSUM Chart for the Phase II data.

Obviously, after 52nd observation a small shift (about 1-σ) occurs in the data. An estimate of new process mean is calculated by Eqn. 8.1.

$$\hat{\mu} = \mu_0 + K + \frac{C_i^+}{N^+} \qquad \text{Eqn. 8.1}$$

$C_i^+ = 3.8$; $N^+=14$; $K=0.47$

$$\hat{\mu} = 16.82 + 0.47 + \frac{3.8}{14} = 17.56$$

The mean of 32-μm %wt has shifted from 16.82 to 17.56. When the milling process is examined, it is realized that there had been an electrical problem on the separator engine in that time period. We would need to make an adjustment on the separator engine.

We can also calculate ARL_o of the process by Eqn. 8.2.

$$ARL = \frac{\exp(-2\Delta b) + 2\Delta b - 1}{2\Delta^2} \qquad \text{Eqn. 8.2}$$

$$\frac{1}{ARL_o} = \frac{1}{ARL_o^+} + \frac{1}{ARL_o^-} \qquad \text{Eqn. 8.3}$$

Setting $\delta^*=0$; then $\Delta = \delta^* - k = 0 - 0.5 = -0.5$, $b = h + 1.166 = 5 + 1.166 = 6.166$, and ARL_o^+;

$$ARL_o^+ \approx \frac{\exp(-2(-0.5)(6.166)) + (2(-0.5)(6.166)) - 1}{2(-0.5)^2} = 938.2$$

By symmetry, $ARL_o^+ = ARL_o^- = 938.2$, the in-control ARL for two sided CUSUM is

$$\frac{1}{ARL_o} = \frac{1}{938.2} + \frac{1}{938.2} \Rightarrow ARL_o = 469.1$$

This result is very close to true value of $ARL_o = 465$. In control condition, an out-of-control signal will be generated about every 470 samples, on the average. There will be a false alarm about every 470 hours on the average.

In the process, the mean shift is about 1-σ, then $\Delta = \delta^* - k = 1 - 0.5 = 0.5$ for the upper one-sided cusum, $\Delta = \delta^* - k = -1 - 0.5 = -1.5$ for the lower one-sided cusum. Then,

$$ARL_o^+ \approx \frac{\exp(-2(0.5)(6.166)) + (2(0.5)(6.166)) - 1}{2(0.5)^2} = 10.76$$

$$ARL_o^- \approx \frac{\exp(-2(-1.5)(6.166)) + (2(-1.5)(6.166)) - 1}{2(-1.5)^2} = 2.4 \times 10^7$$

$$\frac{1}{ARL_1} = \frac{1}{10.76} + \frac{1}{2.4 \times 10^7} \Rightarrow ARL_1 \approx 11$$

This means that about 11 points must be plotted before a point indicates an out-of-control condition.

The average time to detect this shift is;

$$ATS = ARL_1 \times h = 10.76 \times 1 = 10.76 \approx 11h$$

8.5.3. EWMA Control Chart

The exponentially weighted moving-average (EWMA) control chart is also applied to the Phase II data to detect 1-σ shifts in the mean. As a first trial, to construct EWMA control chart, λ and L are chosen as 0.4 and 3.05 respectively (Figure 8.10).

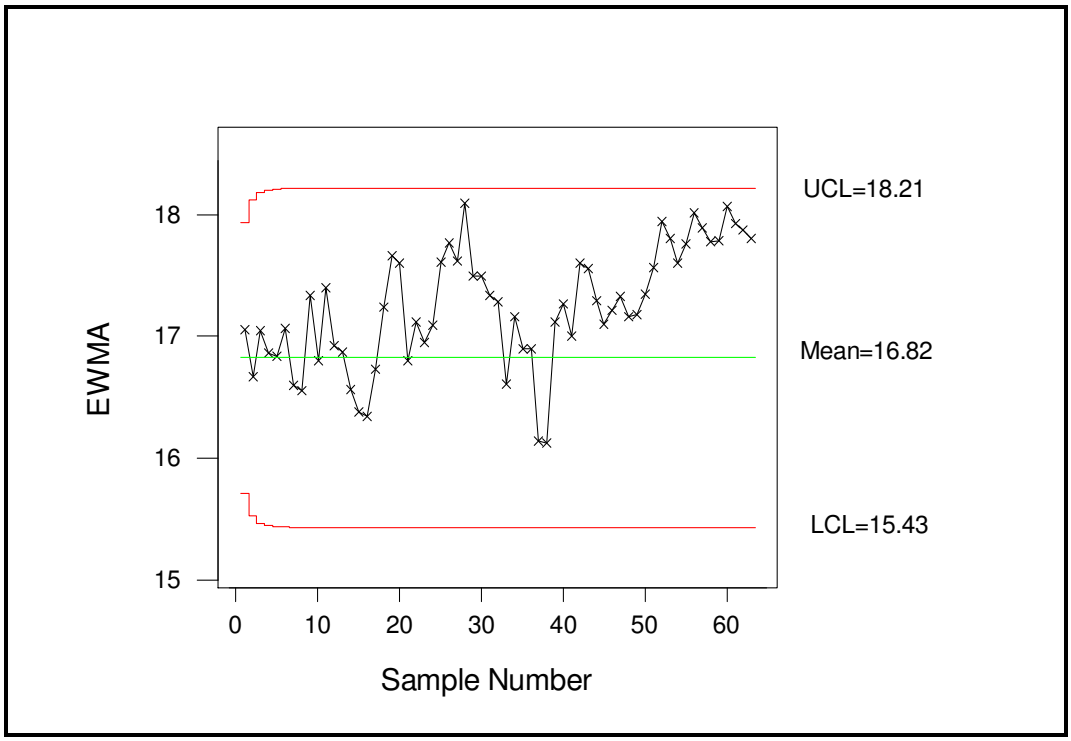

Figure 8.10. EWMA Chart for the Phase II data (λ=0.4 and L=3.05).

As seen from the Figure 10, the CUSUM cannot detect the small shift in this case where λ and L are 0.4 and 3.05 respectively. In order to improve the sensivity of the CUSUM chart, λ and L are chosen as 0.2 and 2.962 respectively in the second trial (Figure 8.11).

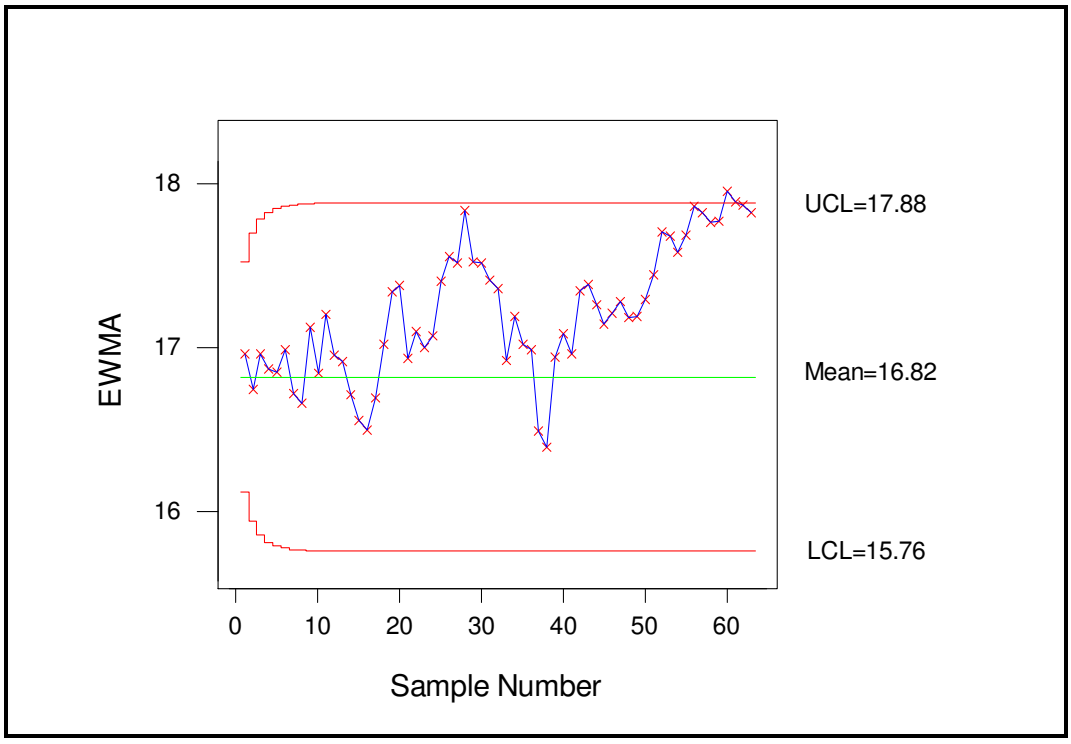

Figure 8.11. EWMA Chart for the Phase II data (λ=0.2 and L=2.962).

Obviously, the CUSUM chart detected the shift, but still there is problem the only one point is out of control condition. To find out whether there exists more out of control points, one more trial is to be applied. Figure 8.12 is constructed with the values: λ=0.05 and L=2.615.

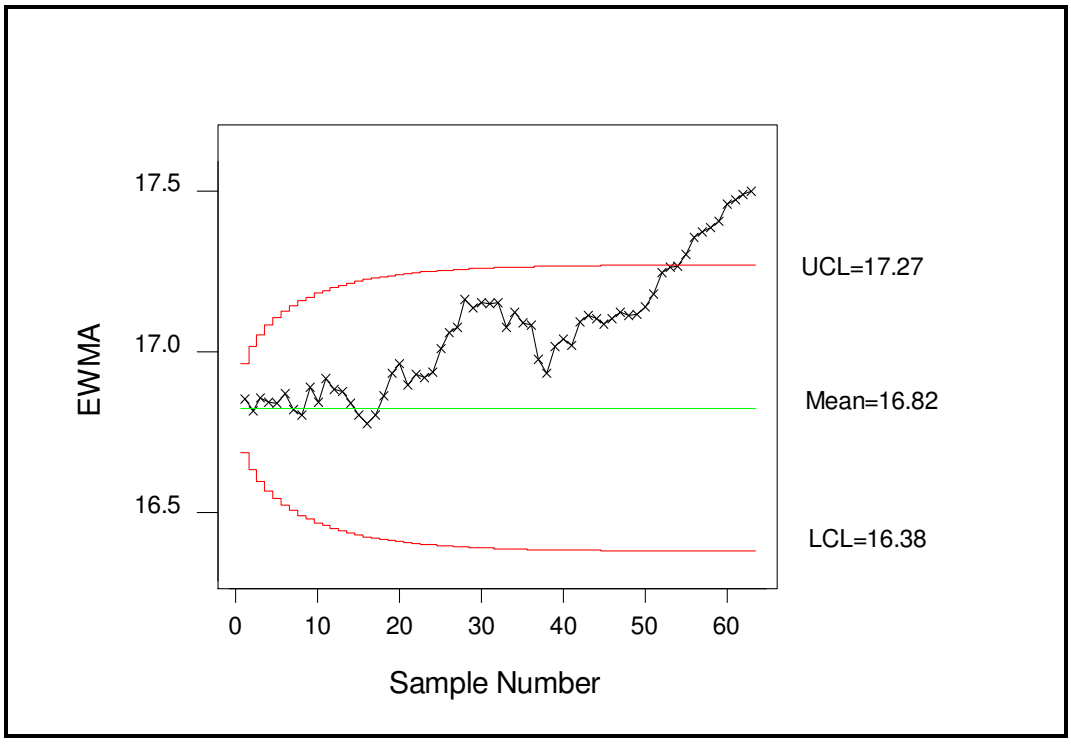

Figure 8.12. EWMA Chart for the Phase II data (λ=0.05 and L=2.615).

The result is very clear that there seen many point in out of control point. This cusum chart is most applicable in the trials. ARL_o is 500 for the EWMA control. In control condition, an out-of-control signal will be generated about every 500 samples, on the average. There will be a false alarm about every 500 hours on the average. This value is higher than CUSUM control ARL_o (470).

Below, ARL values of these EWMA charts are given for 1-σ shifts.

Table 8.4. ARL values for the trials.

Parameters	L = 3.054 λ=0.4	L = 2.962 λ=0.2	L = 2.615 λ=0.05
ARL	14.3	10.5	11.4

As seen from the Table 8.4, the first case has highest ARL_1 that provides the control chart. ARL_1 (10.5) of the case where λ=0.2 and L=2.962 and ARL_1 (11.4) of the case where λ=0.05 and L=2.615 are very close to each other. This makes the EWMA chart with λ=0.05 and L=2.615 best for detecting the small shift in the process data.

This means that about 12 points must be plotted before a point indicates an out-of-control condition.

The average time to detect this shift is;

$ATS = ARL_1 \times h = 11.4 \times 1 = 11.4$

8.5.4. Moving Average Control Chart

After applying I-MR, CUSUM and EWMA control charts, Moving average control chart is to be used for monitoring the process data. MA (Figure 8.13) is constructed by using w (span) as 5.

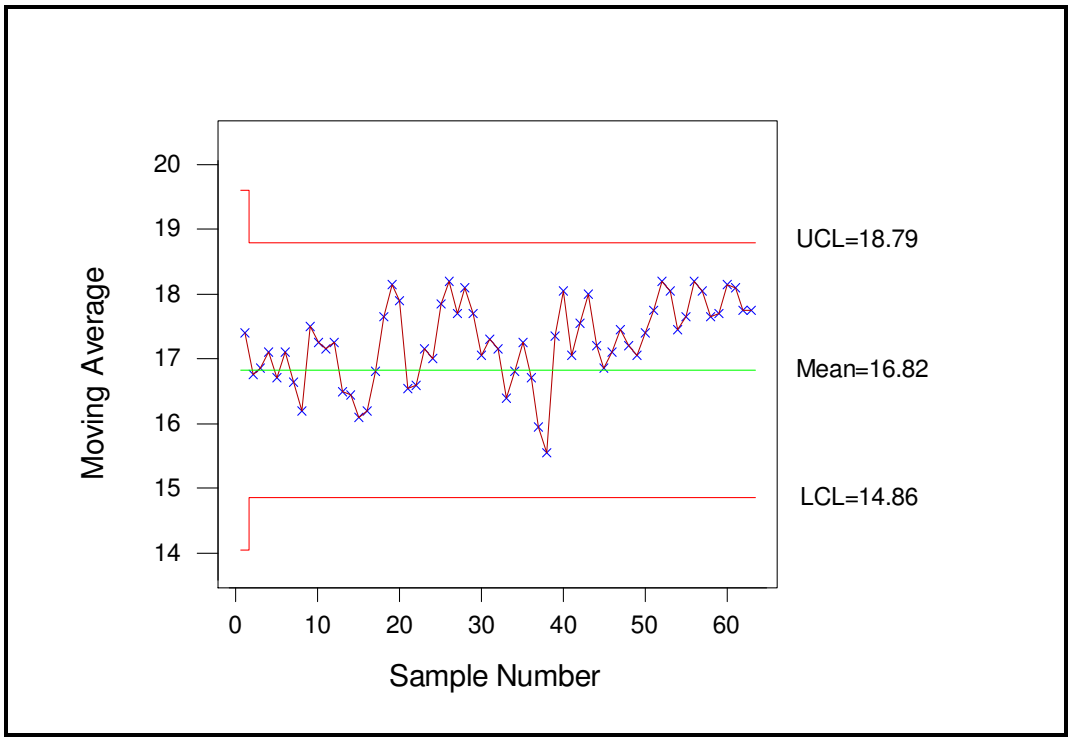

Figure 8.13. MA Chart for the Phase II data.

As I-MR control chart, MA control chart is not effective to detect the 1-σ shift in the process mean.

8.6. Process Capability Analysis for Phase II

Analysis of out-of-control situations needs to be addressed in order to improve the stability and capability of the process. Periodic review of the specifications in relation to the process capability should be conducted on a regular basis.

Figure 8.14 shows that the process capability has deteriorated during the monitoring period to Cp=0.92 and Cp_k=0.71<1, which indicates the potential risk for unacceptable 32-µm fineness has increased from approximately 1992 ppm to approximately 17319 ppm. The probability of rejection is 0.88 %, which means the environmental risk is much higher than it was during the initial baseline period. Corrective measures need to be taken to prevent future non-compliances.

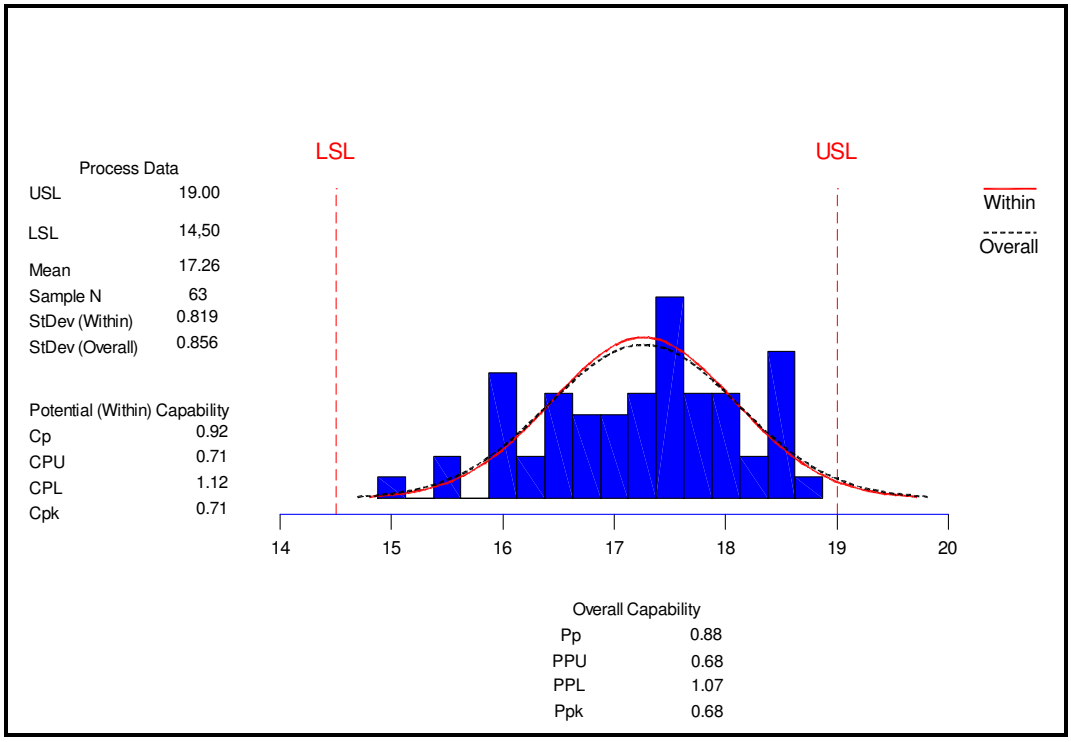

Figure 8.14. Process capability analysis for Phase II data.

CHAPTER 9

CONCLUSION

In this study, portland cement milling process was to be modelled by using cement fineness (32-µm) % wt, which has effect on the hydration rate and thus the setting time, the rate of strength gain, as an output and operational parameters such as revolution (%), falofon (%) and elevator amperage (A). Two combined modelling studies were performed using 2004 Portland cement milling data: ANN and Fuzzy logical approach.

First, the ANN on MatLAB® was applied by using operational parameters (revolution "%", falofon "%" and elevator amperage "A"). 120 data points were used to train the model. It was found that the training resulted with a high R^2=0.86. The performance of the training was also seen in the predicted data versus actual data plot and residuals versus fitted values plot. This allowed us to reach the optimal network that minimizes the error associated with testing data.

The other 35 data points were used to test the model. It was obvious that the model's ability to predict the 32 µm of fineness was successful (R^2=0.85). In spite of some negligible points where the predicted values showed some deviation from the actual fineness data, the performance of the model was good in the predicted versus actual data plot.

The response surfaces constructed by ANN model were used to figure out the Mamdani-type fuzzy rule set in the fuzzy model on MatLAB®. In general, it was realized that increasing the revolution level decreased the fineness, while the falofon % and elevator amperage were kept constant. Furthermore, increasing falofon level, which means that mill feed is increased, increased the fineness level, as the other parameters were kept constant. Similarly, increasing the elevator amperage, which means that the feed to the separator is increased, increased the fineness level.

Finally, the view of rule set and start-up, which were used to predict 32-µm fineness of cement, were obtained. The predicted 32-µm Fineness % wt data followed the actual 32-µm Fineness % wt values with small deviations that the model had a minimum error of 0 % and maximum error of 6.875 %. Also, AAPE of the model is

2.764 %, which shows the performance of the model was good. In fuzzy modeling, the results were not as good compared to ANN. The model had an R^2=0.76 which was lower than ANN's. About 24 % of the total variation could not be accounted for. Performance of the fuzzy model was therefore lower than the ANN model. The fuzzy model, however, is more user friendly, more explicit and easier to construct compared to the ANN model in which the process is a black box.

The extreme values of the targeted fineness, on the other hand, could not be obtained from the model. This was to be expected because the model was conservative and needed more extreme training data to learn the extremes. This was possibly due to other parameters such as C_3S, grindability, moisture that could not be measured every hour because of time and cost constraints. However, it is obviously seen the utility of the ANN and Fuzzy Models created in this study is in the potential ability of the process engineers to control processing parameters to accomplish the desired cement fineness levels.

In the second part of the study, a detailed quantitative procedure for monitoring and evaluating cement milling process performance was described. For statistical monitoring of the process data, an historical data is used. The control limits mean of the process and standard deviation were established. It was also observed that the process data follow a normal distribution. The capability analysis of the historical data after elimination of the out-of-control point supported the results.

After establishing trial control limits, control charts (I-MR, CUSUM, EWMA, AM) were applied to the process data for detecting any shift. It found that the ability of the I-MR control chart and AM control chart to detect small shift is very poor. CUSUM control chart showed good performance to detect the small shift. The mean of 32-μm fineness, %wt, had been shifted from 16.82 to 17.56. When the milling process was examined, it was realized that there had been an electrical problem on the separator engine in that time period. In addition to detecting this small shift, it was realized that there would be a false alarm about every 470 hours on the average in case of using CUSUM control chart. Furthermore, to detect one standard deviation shift, about 11 points are to be plotted. For constructing EWMA control chart, three trials of parameters were applied. Using L=2.615 and λ=0.05 gave best result such that EWMA control chart detected all shifted points. Moreover, ARL_1 value was slightly higher than CUSUM control chart though ARL_o was higher than CUSUM's. However, the sampling

time is very high to detect the shifts. The optimum sampling time is to be found for high quality of the cement.

As a result, we can easily say that the CUSUM and EWMA can be used in the cement milling process monitoring to detect small shifts in the 32-μm fineness, %wt, mean in shorter sampling time interval.

CHAPTER 10

RECOMMENDATION FOR FUTURE WORK

In this study, fuzzy logic model, which was constructed to model the portland cement milling process by operation parameters, had an correlation coefficient of 0.85. Remaining part, which could not be explained by the model, contains some factors affecting on the cement milling process.

Grindibility of clinker and grindibility of additive material are the major affecting parameter on the milling process as a raw material property. The grindibility of the solids (work index) is to be measured by the help of Bond Mill. Also, unknown size distribution of the clinker feed is another parameter that results an error in the model. These parameters are to be observed in the local plant periodically in order to get better control fineness of cement.

The fuzzy logic model generated in this study can be subjected to sensitivity analysis for observation of the effects of processing parameters on the 32-μm fineness (% wt) of portland cement. Such a study would provide a visual control tool for operators in cement plants. In addition to this, a further study can be done to adapt the model to monitor and control the production process in the local plant.

REFERENCES

Akkurt, S., Akyol, B., Ozdemir, S., Tayfur, G. 2003. "The use of GA–ANNs in the modelling of compressive strength of cement mortar", *Cement and Concrete Research,* Vol. 33, p. 973.

Akkurt S., Tayfur, G and Can, S. 2004. "Fuzzy logic model for the prediction of cement compressive strength", *Cement and Concrete Research*. Vol. 34, p. 1429.

Ankovic, A., Valery W. and Davis, E. 2004. "Cement grinding optimisation", *Minerals Engineering,* Vol. 17, p.1075.

Austin L. G., Luckie P. T. and Wightman, D. 1975. "Steady-state simulation of a cement-milling circuit", *International Journal of Mineral Processing*, Vol. 2, p. 127.

Bogue, R. H., 1955. *The Chemistry of Portland Cement*, (Reinhold Publishing Corp., New York.)

Boulvin M., Wouwer, A.V. 1997. "Modeling, simulation and evaluation of control loops for a cement grinding process", Proceedings of European Control Conference, Brussels-Belgium, Paper TH-E-H4.

Breusegem, V., Pierpont, V. 1996. "An industrial application of multivariable linear quadratic control to a cement mill circuit", *IEEE Trans. Ind. Appl*. Vol. 32, p. 670.

CEMBUREAU Working Group of cement technology experts,1999. *Best Available Techniques for The Cement Industry*, (CEMBUREAU:The European Cement Association, Belgium), p.26.

Czernin, W., 1980. *Cement Chemistry and Physics for Civil Engineers*, (Bauverlag, Berlin), p. 11.

Demuth, H., Beale, M., 2004. *Neural Network Toolbox User's Guide*, (The MathWorks, Inc., USA).

Jantzen, J., 1999. "Design of fuzzy controllers", Technical Report, Department of Automation, Technical Univ. of Denmark, No:98- E864.

Hideyuki TAKAGI, 1990. "Fusion Technology of Fuzzy Theory and Neural Networks, Fuzzy Logic and Neural Networks", Conference Izzuka '90, Izzuka-Japan, (July 24).

Kilir, G.J., Fogel, T.A., 1988. *Fuzzy Sets, Uncertainty and Information*, (Prentice-Hall, New York).

Kosko, B., 1992. *Fuzzy Thinking: The New Science of Fuzzy Logic*, (Hyperion, New York.)

Magni, L., Bastin, G., Wertz, V., 1999. "Multivariable nonlinear predictive control of cement mills", *IEEE Trans. Contr. Syst. Technol*. Vol. 7, p. 502.

McNeill, F.M., Thro, E., 1994. *Fuzzy Logic: A Practical Approach*, (Hyperion, New York.).

Mindess, S. and Young, J. F., 1981. *Concrete*, (Prentice-Hall, Inc., Englewood Cliffs).

Munakata, T., 1998. *Fundamentals of the New Artificial Intelligence: Beyond Traditional Paradigms*, (Springer-Verlag, New York.)

Powers, T. C., Copeland, L. E., Hayes, J. C., and Mann, H. M., 1954. "Permeability of portland cement paste", *ACl Journal Proceedings*, Vol. 51 (3), p. 285.

Powers, T.C., 1985. "Guide to the selection and use of hydraulic cements", ACI Committee 225R.

Taylor, H.F.W., 1990. *Cement Chemistry*, (Academic Press, New York), p.79.

Topalov, A. V., Kaynak, O., 2004. "Neural network modelling and control of cement mills using a variable structure systems theory based on-line learning mechanism", *Journal of Process Control*, Vol. 14, p. 581.

Topalov, A.V., Kaynak, O., 2004. "Neural network modeling and control of cement mills using a variable structure systems theory based on-line learning mechanism", *Journal of Process Control*, Vol. 14, p. 58.

Sen, Z., 1999. "Fuzzy Modeling in Engineering", Class Notes, Civil Engineering Faculty, Istanbul Technical University, Istanbul, Turkey.

Sen, Z., 1998. "Fuzzy algorithm for estimation of solar irradiation from sunshine duration", *Sol. Energy*, Vol. 63 (1), p. 39.

WEB_1, 2004 FHWA's web site, 11/05/2004. http://www.fhwa.dot.gov/infrastructure/materialsgrp/cement.html.

Zadeh, L., Kacprzyk, J., 1992. *Fuzzy Logic for the Management of Uncertainty*, (Wiley, New York).

APPENDIX A
TABLES

Table A.1. Data used in ANN and Fuzzy modelling (Çimentaş).

	OUTPUT	INPUTS		
Obs. No	**Fineness (32 µm) (%)**	**Revolution (%)**	**Falofon (%)**	**Elevator Amp. (A)**
1	17.2	63	93	96
2	17.8	64	94	95
3	14.3	68	94	66
4	16.2	67	95	73
5	17.4	63	94	75
6	14.3	66	92	71
7	17.1	65	94	70
8	16.1	65	94	71
9	15.8	67	92	70
10	14.7	67	93	95
11	14.3	66	92	71
12	17.8	64	94	96
13	14.8	65	92	71
14	15.3	63	92	71
15	15.6	65	93	74
16	16.5	65	94	88
17	15.2	67	93	66
18	16.5	67	96	97
19	15.2	64	93	72
20	18	63	95	76
21	17.5	64	94	94
22	16.8	67	96	98
23	16.5	65	94	86
24	16.2	65	93	73
25	16.1	64	96	90
26	14.6	67	94	96
27	15.9	64	96	91
28	16.5	67	96	73
29	16.5	65	93	73
30	16.4	64	95	88
31	15.8	68	95	72
32	15.5	64	92	70
33	18.5	64	96	84
34	16.7	65	93	70
35	17	64	94	69
36	18	65	94	89
37	16.5	65	93	73
38	15.6	63	92	66
39	17.5	64	93	75
40	16.8	66	95	71
41	17.5	63	92	93
42	16	65	92	66
43	15.4	68	93	92
44	17.8	63	93	95
45	16.1	65	94	71
46	16.3	65	94	69
47	16.8	66	94	74

Table A.1 (Cont.). Data used in ANN and Fuzzy modelling (Çimentaş).

	OUTPUT	INPUTS		
Obs. No	Fineness (32 µm) (%)	Revolution (%)	Falofon (%)	Elevator Amp. (A)
48	16.4	64	95	88
49	14.6	67	93	92
50	15.3	67	93	75
51	17.5	63	92	73
52	15.6	68	94	74
53	16	64	93	75
54	16.8	63	93	68
55	17.5	63	95	71
56	15.1	67	93	67
57	16.6	66	94	66
58	16.2	68	94	71
59	15.4	64	93	68
60	14.2	67	92	69
61	15.1	67	95	68
62	16.5	65	93	73
63	15.8	68	94	71
64	17.2	64	94	66
65	14.4	67	93	93
66	14	67	93	68
67	16.2	65	92	91
68	17.4	65	95	71
69	16	67	95	96
70	17.1	63	93	74
71	14.5	67	94	94
72	16.5	66	95	72
73	17.8	64	94	95
74	15.4	67	93	96
75	15.5	67	92	90
76	18.4	63	94	75
77	16.5	65	94	85
78	18.2	65	94	88
79	16.6	65	94	71
80	16.1	65	94	73
81	17.1	65	95	82
82	17.1	63	93	95
83	16.7	65	94	71
84	17.5	64	94	96
85	17.5	65	93	71
86	16.6	64	95	85
87	17.5	65	94	72
88	17.1	63	95	72
89	16	65	92	66
90	16.5	65	95	71
91	16.3	66	94	71
92	16.5	65	94	86
93	16.4	65	94	72
94	17.5	63	95	71

Table A.1 (Cont.). Data used in ANN and Fuzzy modelling (Çimentaş).

	OUTPUT	INPUTS		
Obs. No	Fineness (32 µm) (%)	Revolution (%)	Falofon (%)	Elevator Amp. (A)
95	16	65	93	69
96	17.6	63	92	73
97	16.3	66	95	67
98	15.6	64	96	69
99	15.3	63	92	67
100	15.6	64	96	69
101	15.2	67	92	72
102	17.1	65	94	70
103	17.8	65	94	72
104	14.2	67	92	69
105	18.4	65	94	68
106	15.4	67	93	75
107	16.7	66	94	73
108	17.3	66	96	68
109	18.1	64	93	69
110	15.4	68	94	75
111	18.3	63	95	75
112	16.5	65	92	69
113	18.3	63	94	75
114	18.3	64	93	72
115	14.1	67	92	68
116	14.5	67	94	76
117	16	67	94	77
118	17.2	65	95	89
119	16.5	66	95	72
120	14.2	68	94	68
121	18.3	63	95	75
122	15.3	67	95	66
123	15.4	68	94	75
124	16.2	67	95	94
125	16.6	66	94	66
126	17.1	63	93	74
127	17.5	64	94	94
128	17	64	94	69
129	14.8	65	92	71
130	17.5	64	94	96
131	18	63	95	76
132	17.3	64	96	72
133	18.2	65	96	89
134	15	67	93	67
135	14.5	65	93	72
136	17.1	63	93	95
137	16.4	66	94	67
138	16.3	66	94	71
139	16.2	65	93	73
140	16.8	66	94	74
141	16.4	65	94	72

Table A.1 (Cont.). Data used in ANN and Fuzzy modelling (Çimentaş).

	OUTPUT	INPUTS		
Obs. No	**Fineness (32 µm) (%)**	**Revolution (%)**	**Falofon (%)**	**Elevator Amp. (A)**
142	17.5	65	94	72
143	16.8	67	96	98
144	17.3	66	96	69
145	17.2	65	95	70
146	18	66	96	88
147	14.1	67	92	68
148	16	67	92	71
149	15.4	68	93	92
150	15.2	67	93	66
151	16	67	94	77
152	16.5	66	95	72
153	15.8	68	95	72
154	16.2	67	95	73
155	16.5	67	96	97

Table A.2. 35 testing data sets for the testing of ANN and Fuzzy logic-based model.

Obs. No	OUTPUT	INPUTS		
	Fineness (32 µm) (%)	Revolution (%)	Falofon (%)	Elevator Amp. (A)
1	18.3	63	95	75
2	15.3	67	95	66
3	15.4	68	94	75
4	16.2	67	95	94
5	16.6	66	94	66
6	17.1	63	93	74
7	17.5	64	94	94
8	17	64	94	69
9	14.8	65	92	71
10	17.5	64	94	96
11	18	63	95	76
12	17.3	64	96	72
13	18.2	65	96	89
14	15	67	93	67
15	14.5	65	93	72
16	17.1	63	93	95
17	16.4	66	94	67
18	16.3	66	94	71
19	16.2	65	93	73
20	16.8	66	94	74
21	16.4	65	94	72
22	17.5	65	94	72
23	16.8	67	96	98
24	17.3	66	96	69
25	17.2	65	95	70
26	18	66	96	88
27	14.1	67	92	68
28	16	67	92	71
29	15.4	68	93	92
30	15.2	67	93	66
31	16	67	94	77
32	16.5	66	95	72
33	15.8	68	95	72
34	16.2	67	95	73
35	16.5	67	96	97

APPENDIX B
FIGURES

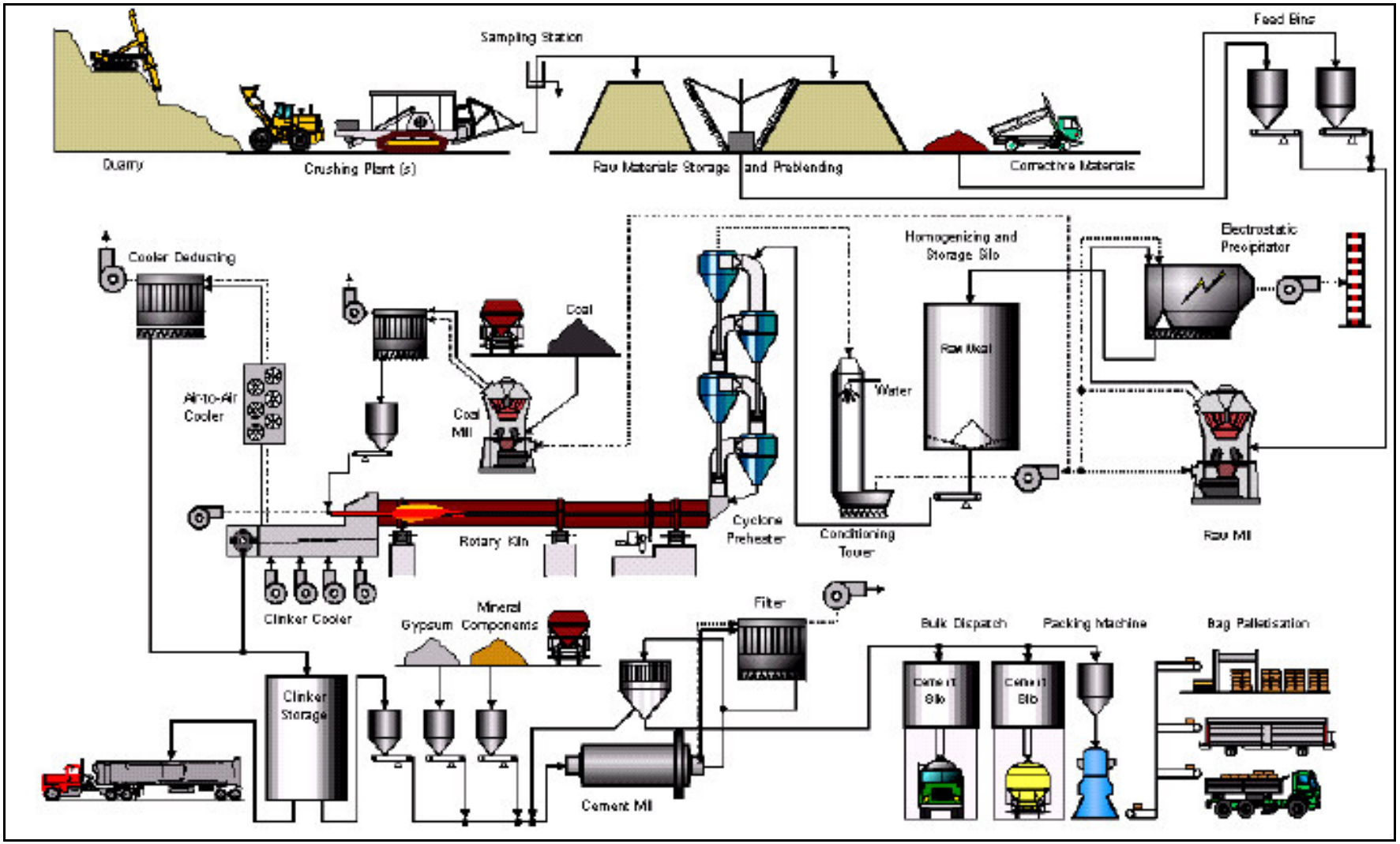

Figure B.1. Production of Cement by the Dry Process (Source: CEMBERNEU 1996).

Figure B.2. Sieve equipment used in the local plant.

Figure B.3. The Ball Mill used in the local plant.

Figure B.4. Polysius® Cyclone Air Separator used in the local plant.

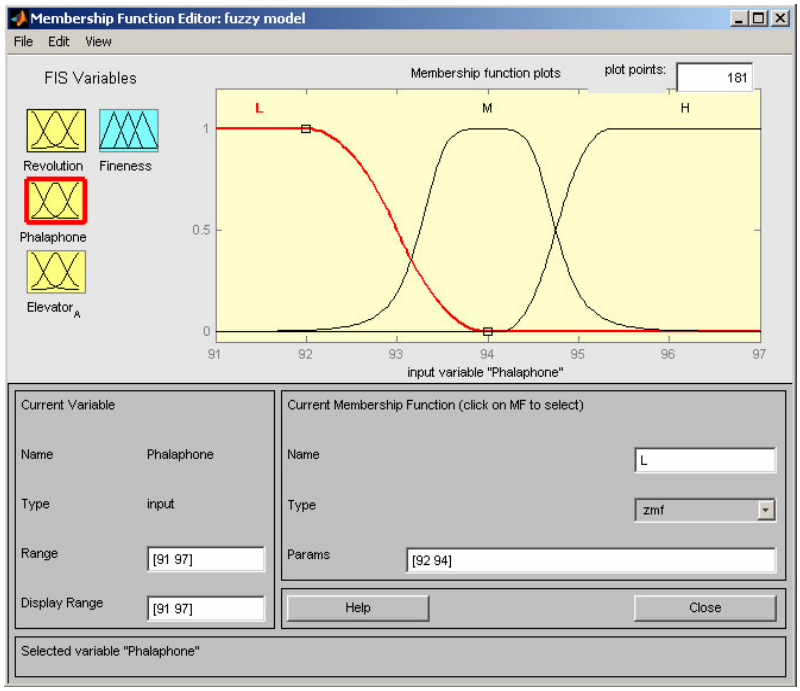

Figure B.5. Membership function of Falafon.

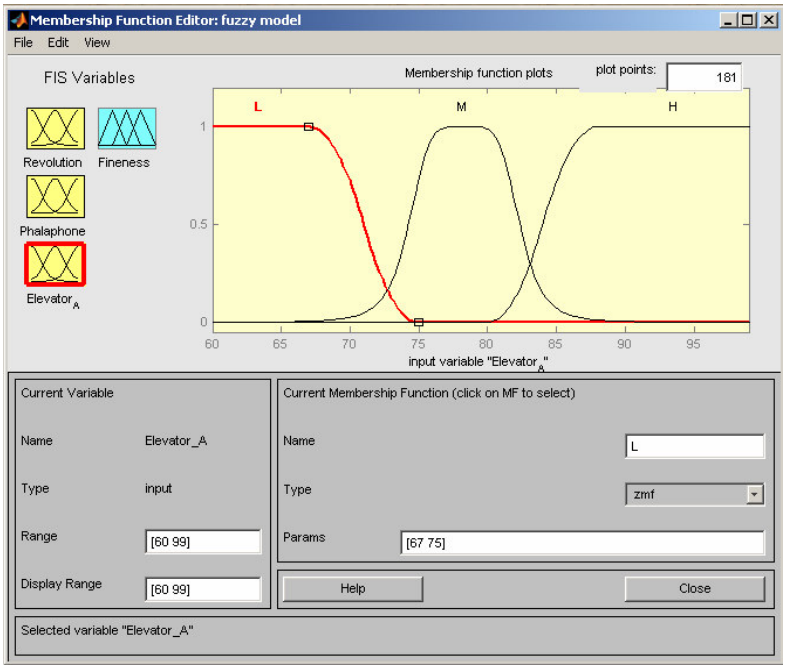

Figure B.6. Membership function of Elevator A.